Max-Planck-Institut
für Meteorologie

REPORT No. 188

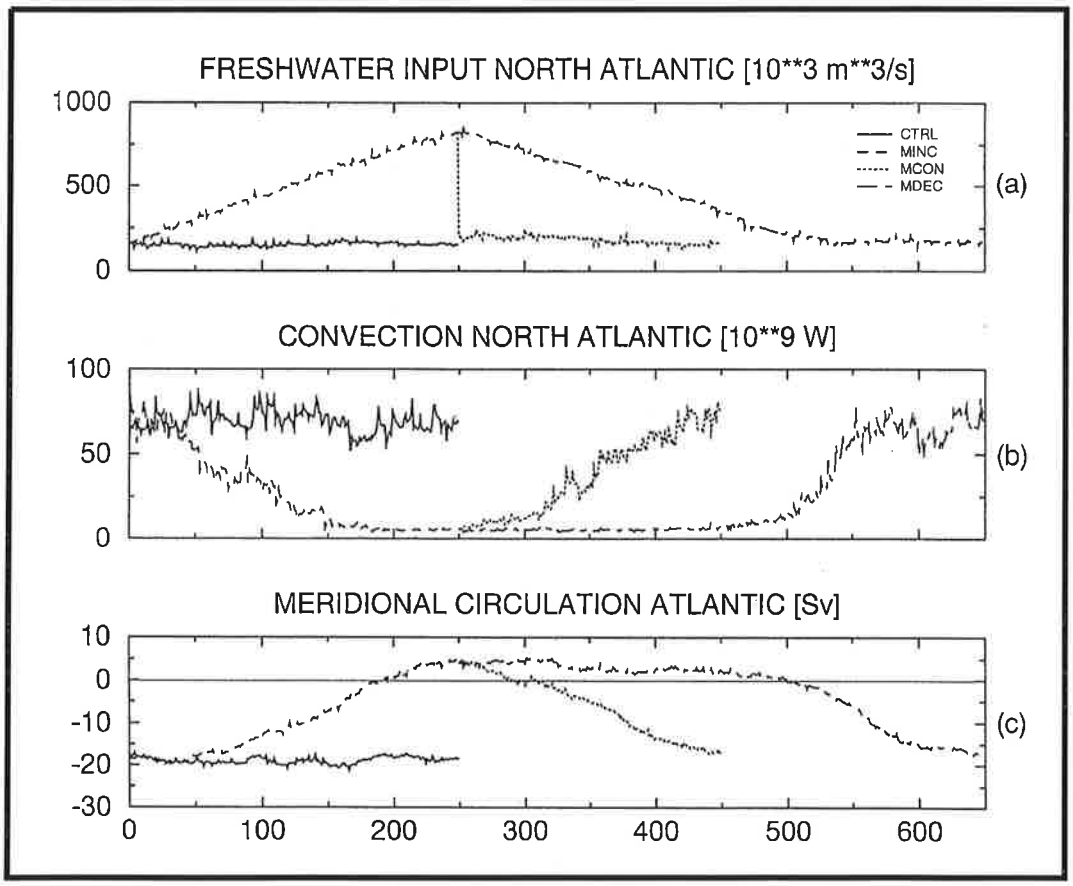

THE STABILITY OF THE THERMOHALINE CIRCULATION IN A COUPLED OCEAN-ATMOSPHERE GENERAL CIRCULATION MODEL

by

ANDREAS SCHILLER · UWE MIKOLAJEWICZ · REINHARD VOSS

HAMBURG, February 1996

AUTHORS:

Andreas Schiller

Max-Planck-Institut
für Meteorologie
now at
CSIRO Division of Oceanography
GPO Box 1538
Hobart TAS 7001
Australia

Uwe Mikolajewicz

Max-Planck-Institut
für Meteorologie

Reinhard Voss

DKRZ
Deutsches Klimarechenzentrum
Bundesstraße 55
D - 20146 Hamburg
Germany

MAX-PLANCK-INSTITUT
FÜR METEOROLOGIE
BUNDESSTRASSE 55
D-20146 Hamburg
F.R. GERMANY

Tel.: +49-(0)40-4 11 73-0
Telefax: +49-(0)40-4 11 73-298
E-Mail: <name> @ dkrz.de

ISSN 0937-1060

The Stability of the Thermohaline Circulation in a Coupled Ocean-Atmosphere General Circulation Model

Andreas Schiller[1,2] Uwe Mikolajewicz[1,4] Reinhard Voss[3]

1: Max-Planck-Institut für Metereologie, Bundesstraße 55, 20146 Hamburg, Germany
2: now at: CSIRO Division of Oceanography, GPO Box 1538 Hobart TAS 7001, Australia
3: Deutsches Klimarechenzentrum, Bundesstraße 55, 20146 Hamburg, Germany
4: corresponding author

Abstract

The stability of the Atlantic thermohaline circulation against meltwater input is investigated in a coupled ocean-atmosphere general circulation model. The meltwater input to the Labrador Sea is increased linearly for 250 years to a maximum input of 0.625 Sv and then reduced again to 0 (both instantaneously and slowly decreasing over 250 years). The resulting freshening forces a shutdown of the formation of North Atlantic deepwater and a subsequent reversal of the thermohaline circulation of the Atlantic, filling the deep Atlantic with Antarctic bottom water. The change in the overturning pattern causes a drastic reduction of the Atlantic northward heat transport, resulting in a strong cooling with maximum amplitude over the northern North Atlantic and a southward shift of the sea-ice margin in the Atlantic. Due to the increased meridional temperature gradient, the Atlantic intertropical convergence zone is displaced southward and the westerlies in the northern hemisphere gain strength. We identify four main feedbacks affecting the stability of the thermohaline circulation: the change in the overturning circulation of the Atlantic leads to longer residence times of the surface waters in high northern latitudes, which allows them to accumulate more precipitation and runoff from the continents, which results in an increased stability in the North Atlantic. This is further amplified by a enhanced northward atmospheric water vapour transport, which increases the freshwater input into the North Atlantic. The colder sea-surface temperatures due to a reduction of northward oceanic heat transport and the increased upwelling (Ekman suction) in the Norwegian Sea in response to an intensified cyclonic circulation decrease the vertical stability. Thus the latter two effects largely compensate for the effects of the first two feedbacks. The windstress feedback stabilizes the present mode of ocean circulation, but has been neglected in almost all studies so far.

After the meltwater input stops, the North Atlantic deepwater formation resumed in all experiments and the meridional overturning returned within 200 years to a conveyor belt pattern. This happened although the formation of North Atlantic deep water has been suppressed in one experiment for more than 300 years and the Atlantic overturning had settled into a circulation pattern with Antarctic bottom water as the only source of deep water. It is a clear indication that cooling and windstress feedback are more effective, at least in our model, than advection feedback and increased atmospheric water vapour transport. We conclude that the present-day type thermohaline circulation – at least in our model – seems to be much more stable than hitherto assumed from experiments with simpler models.

ISSN 0937-1060

1 Introduction

Since the discovery of the ocurrence of ice ages, people have speculated on the cause of these extensive climate changes. Nowadays it is widely accepted that the transitions between glacials and interglacials are caused by long periodicities in the orbit of the earth around the sun and resulting changes in solar irradiance (Milankovitch, 1930). While this hypothesis might explain the long periodic components of past climate changes and their almost regular behaviour, it cannot explain the large amplitudes of the observed climatic cycles; there must be strong feedback processes in the climate system itself amplifying and modulating the forcing. As well, the geological records show some strong climatic events with large temperature changes happening within a few decades. The most prominent example is the Younger Drays cold event during the last deglaciation about 13,000 years ago, when Europe and the North Atlantic experienced a sudden return to almost glacial conditions, which lasted for about 1300 years (Mayewski et al., 1993). Other examples are the "Dansgaard-Oeschger" events, first found in Greenland ice cores during glacial periods (Dansgaard, 1985), and the "Heinrich" events, which are connected with outflow of icebergs into the North Atlantic (Heinrich 1988, Broecker et al., 1992). Events of both types are recorded in sediment cores all over the northern North Atlantic and also in the new Greenland ice cores (Bond et al., 1993).

It has often been speculated (e.g. Rooth, 1982) that changes in the thermohaline circulation of the ocean and associated changes in oceanic heat transport might be responsible for these large climate changes. The speculations are built on the fact that – at least in certain parameter regimes – ocean models can have multiple steady states of the thermohaline circulation (especially in the North Atlantic). One state resembles the present overturning pattern with strong formation of North Atlantic deep water (NADW) and an associated oceanic northward heat transport of about 1 PW; another steady state is similar to the thermohaline circulation of the Pacific but with much weaker northward heat transport. Stommel (1961) showed the possibility of multiple steady states of the thermohaline circulation in a simple two-box model for parameter regimes, where sea surface temperature (SST) anomalies are damped out rather fast by feedback processes with the atmosphere, while anomalies of sea surface salinity are not felt by the atmosphere, which is thus not able to damp them. Later, Bryan (1986) showed in an idealized setup that ocean general circulation models (OGCMs) also had this potential when driven with so-called traditional mixed boundary conditions (strong relaxation of the uppermost level temperature towards climatological SST and a freshwater flux for salinity, which is often replaced in models with rigid lid by a "salt flux"). Manabe and Stouffer (1988, MS88 hereafter) found also multiple steady states in their coupled ocean-atmosphere general circulation model (OAGCM) with annual mean insolation.

Due to the cost of the coupled OAGCMs, later experiments were mainly carried out with OGCMs with traditional "mixed boundary conditions". Maier-Reimer and Mikolajewicz (1989, referred to below as MM89) showed that the addition of small amounts of meltwater to the North Atlantic was sufficient to cause a transition from the present mode of ocean circulation with strong formation of NADW to another one without NADW formation. Furthermore, they showed that the stability of the thermohaline circulation strongly depended on the location of the freshwater input, thus supporting the hypothesis that the Younger Dryas was caused by meltwater input from the Laurentide ice sheet (Rooth, 1982, Broecker et al., 1985). The problem of multiple steady states was mostly studied under mixed boundary conditions (e.g. Marotzke and Willebrand, 1991, Mikolajewicz et al., 1993, Hughes and Weaver, 1994; see Weaver and Hughes, 1992, or Rahmstorf et al., 1995, for a review). In realistic

setups (topography, forcing fields) it nearly always turned out that the mode without NADW was much more stable and more likely to occur than the present mode of ocean circulation, which cannot explain why the ocean has been in a mode with NADW during most of the deglaciation period.

The unrealistically weak stability of the present mode of the thermohaline circulation in OGCMs was found recently to be an artefact of the use of "mixed boundary conditions". The strong relaxation to a constant temperature does not adequately represent the atmospheric temperature feedback, so that changes in oceanic heat transport cannot compensate at least partly for the density changes due to salinity. The stability of the modes of the thermohaline circulation was shown to depend quite critically on the formulation of the upper boundary condition for temperature (e.g. Nakamura et al., 1994, in a simple box model; Wright and Stocker, 1993, in a 2.5D ocean model; Zhang et al., 1994, Mikolajewicz and Maier-Reimer, 1994 – referred to below as MM94 – and Rahmstorf and Willebrand, 1995, for OGCMs). The present mode of the thermohaline circulation seems to be becoming more and more stable as the description of the atmospheric feedbacks becomes more realistic. Because a complete description of all potential atmospheric feedback processes associated with the changes in oceanic overturning can only be simulated in a coupled OAGCM, we use one to investigate in this paper the stability of the thermohaline circulation to meltwater input.

The question of the stability of the thermohaline circulation might be relevant not only to explain past climate changes but also for anthropogenic climate change. Coupled OAGCMs show the thermohaline circulation of the Atlantic weakens markedly in response to a greenhouse warming (e.g. Manabe and Stouffer, 1990, Cubasch et al., 1992). This weakening is a transient behaviour for a CO_2-doubling, but a permanent feature for quadrupled atmospheric CO_2-concentrations (Manabe and Stouffer, 1993). In greenhouse simulations, the weakening of the overturning in the Atlantic and the resulting weaker oceanic heat transport compensated in the northern North Atlantic and in western Europe at least partly for the radiative forcing, ending up with a minimum of the warming (or even a slight cooling) in these areas (see e.g. Gates et al., 1992, for a review).

This paper will investigate one of the main potential mechanisms of climate change inherent in the atmosphere-ocean subsytem of the present climate systems. Therefore we will limit ourselves to investigating the response of the model to rather idealized forcing scenarios. This paper is not intended to give an exact picture of any geological event (e.g. the Younger Dryas period), though the results might be applicable to interpreting past climate changes. Thus vegetation, distribution of glaciers, composition of the atmosphere etc. are all given present values.

In the ocean there are several relevant time scales. In the most important one for our study, the mixed-layer, the sea-ice distribution and the atmospheric circulation adapt to a given oceanic heat transport. This time scale is typically of the order of 10^1 years. The longest time scale involved is the renewal of the properties of the deep ocean. This time scale is of the order of 10^3 years, as NADW needs more than 1000 years to well up in the North Pacific again. Thus the time scale for a coupled model to reach a statistical equilibrium (or a state close to it) is typically a couple of thousand years, although it could be longer if the old deepwater is denser than any of the newly formed, and conditions become stagnant. As the coupled OAGCMs even in coarse resolution are still very expensive, we could not continue our experiments until a state of equilibrium was reached. In the ocean-only experiments presented in Maier-Reimer et al. (1993) the principal overturning pattern of the Atlantic usually showed up much earlier (within a few centuries) and we believe this to be true in case

of the coupled model as well. We must stress, however, that we cannot exclude the possibility that the circulation pattern changes later. Moreover, it is not known, whether the real ocean has ever reached such an equilibrium.

The paper is organized as follows: in section 2 the ECHAM3/LSG coupled ocean-atmosphere model and its climate are briefly described and the periodically synchronously coupling technique explained; in section 3 the results of our meltwater release experiments are given and the important feedbacks identified; in section 4 the results are discussed, and in section 5 the results are summarized.

2 The coupled ocean-atmosphere model

2.1 Model description

A coupled ocean-atmosphere general circulation model was used to perform the experiments presented in this paper. The atmosphere component was the spectral atmospheric general circulation model ECHAM3 (Roeckner *et al.*, 1992) with T21 horizontal resolution and 19 layers in the vertical. The prognostic variables are vorticity, divergence, temperature, surface pressure, humidity and cloud water. The model contains parameterizations of radiation, cloud formation, precipitation, convection, and vertical and horizontal diffusion. The annual and daily cycles of the solar radiation are included.

The oceanic component of the coupled model was the Large-Scale-Geostrophic (LSG) general circulation model (Maier-Reimer et al., 1993) with a horizontal resolution similar to the Gaussian grid of the T21 atmospheric model (5.6° x 5.6°), but on an "E"-type grid (Arakawa and Lamb, 1977) and 11 layers in the vertical. A simple sea-ice model is included. The model is based on the standard set of equations used in OGCMs, but additionally the advection of momentum is neglected is this model. The model has a free upper surface. Due to the implicit formulation of the model, a time step of one month can be achieved without stability problems. The model is especially designed for long integrations in a coarse resolution.

The atmosphere and the ocean models are coupled by the fluxes of heat, mass (freshwater) and momentum (wind stress). These fluxes, which are calculated in the atmospheric model, are taken as forcing for the ocean model. The sea-surface temperature (SST) and the ice thickness of the oceanic model component serve as the lower boundary conditions for the atmosphere model. To reduce the climate drift of the coupled model the flux correction method is applied (Sausen et al., 1988). It couples the atmosphere and ocean by the anomalies of the fluxes computed relative to the equilibrium states of the uncoupled models. The constant flux correction terms are in some places quite large, but they are typically of the same magnitude as the flux correction terms from other coupled models with similar resolution (cf. Gates et al., 1993).

The surface temperature field over ocean points that serves as a boundary condition for the atmosphere model consists of the SST distribution computed by the ocean model (temperature of the uppermost level) and a correction term that depends only on the seasonal cycle. For ice-covered ocean grid points, the surface temperature of the sea-ice is computed in the atmosphere model by balancing long- and shortwave radiation, sensible and latent heat flux, and the conductive heat flux through the ice (which is assumed to be inversely proportional to the sea-ice thickness).

For processes with typical time scales of a few decades and longer, the atmosphere gen-

erally is in statistical equilibrium with SST and sea-ice distribution. Thus, the atmospheric forcing for the ocean will vary only on shorter time scales (interannual and shorter).

As the atmosphere model uses the overwhelming part of the total computer time, it is tempting to integrate the atmosphere during only part of the coupled simulation. Such a technique was proposed by Gates (Schlesinger, 1979) under the term "periodically-synchronous" coupling. In a periodically synchronously coupled model, periods with quasi-simultaneous integrations of the ocean and atmosphere model components (synchronous coupling) alternate with ocean-only integrations. During the ocean-only periods the forcing is calculated from previous synchronously coupled periods. This method is significantly cheaper than integrating the fully synchronously coupled model, and the results are similar, if one is interested only in the long-term behaviour of the system and not in the interannual variability (Voss and Sausen, 1996).

In our setup, the atmospheric model ECHAM3 used about 90% of the computer time of the synchronously coupled model; its temporary switch-off during the ocean-only periods reduced the computer time substantially. For the following experiments we chose synchronous periods of 15 months and ocean-only integrations of 48 months. As no atmospheric feedback is possible during the ocean-only periods, SST and sea-ice anomalies that occur during these pure flux-driven periods are not damped. With this choice of integration periods, the model drift in the ocean-only periods was small and the model stayed within the path given by the synchronously coupled model. This coupling technique reduced the computer time approximately by a factor of 3 compared to the purely synchronously coupled model.

All experiments were started from the model state reached after an integration over 115 years, which was performed with purely synchronous coupling under present-day forcing conditions. More details of the coupled model and the periodically-synchronous coupling technique are given in Voss *et al.* (1996) and in Voss and Sausen (1996).

If not stated differently, all pictures show the mean values of decades computed from the last decade of the experiment relative to the fields derived from the respective time period of the control run. The assumption is that changes in the control run represent a spurious drift or a component of the natural variability that is common to all experiments (Cubasch et al., 1992). The climate response is then defined as the instantaneous difference between the actual freshwater disturbance experiment and the control run at the same time instance.

Except for the timeseries, the diagrams were computed from a synchronous integration over the last decade of the experiments. The short synchronous integrations were performed to enable us to evaluate the results of the atmospheric component of our model and to test the influence of the periodically synchronous coupling technique. No serious differences were found between the results of the synchronous and the periodically-synchronous coupled model runs.

All horizontal variables of the atmosphere were interpolated onto the grid of the ocean model and are shown within the frame of the ocean model. In the atmosphere model one grid point corresponds to two grid points of the ocean model.

2.2 The climate of the control experiment

This subsection gives a brief overview of the final state of the control experiment CTRL (last decade of 250 years of model integration). The pictures presented here serve as a reference for the subsequent sections.

Figure 1 shows the zonally averaged meridional overturning stream function of the At-

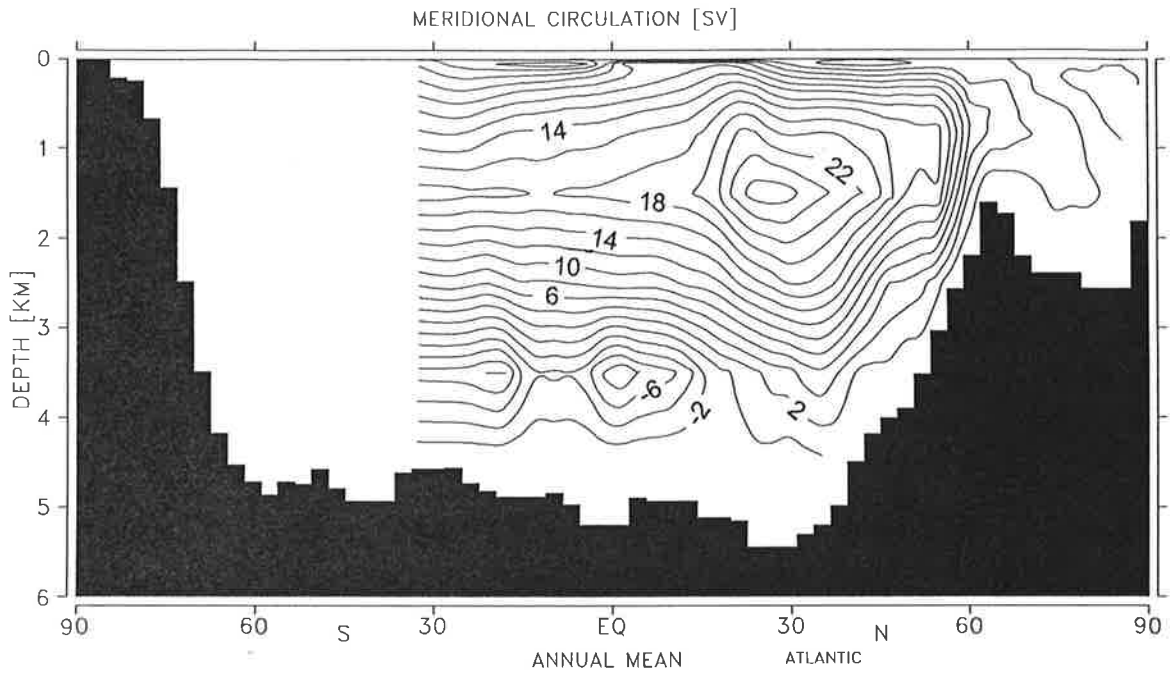

Figure 1: Zonally integrated meridional mass transport streamfunction of the Atlantic. Results are for the final decade (years 241-250) of control run (Exp. CTRL). Positive values denote clockwise rotation. C.I.: 2×10^6 m^3/s.

lantic. The dominant feature is the vigorous overturning cell consisting of the northward flow of warm and saline water near the surface, the area with descending motion and deep convection around 50° to 60°N, and the southward return flow as NADW. The NADW sinks down to a core depth between 2000 and 3000 m, whereas the Antarctic Bottom Water (AABW) penetrates northward into the abyssal Atlantic up to 20°N. The model's circulation follows the pattern derived from observations (e.g. Gordon, 1986, Broecker, 1991, Rintoul, 1991, Schmitz, 1995), but it seems to slightly overestimate the strength of this circulation. The model climate has an outflow of about 18 Sv of NADW to the Southern Ocean (at 30°S) which compares reasonably well with estimates from inversion of distributions of temperature, salinity and passive tracers (e.g. Gordon, 1986, gives 13.5 Sv). According to Figure 2 the dominant areas of deep convection and water-mass formation in the model are concentrated around Antarctica (AABW) and in the North Atlantic (NADW), in particular in the Irminger Sea and in the Greenland-Iceland and Norwegian Sea (GIN-Sea). It is widely accepted for the real ocean (e.g. Killworth, 1983) that NADW forms in the GIN-Sea and the Labrador Sea. In the Southern Ocean the centers of deep water production are the Weddell and the Ross seas.

The zonally and annually averaged meridional circulation of the atmosphere is realistically simulated by the model. Figure 3 compares the mean vertical circulation of the control experiment with the ECMWF (European Centre for Medium Range Weather Forecasts) analysis from 1981 to 1993, interpolated into the model grid. The annual mean circulation pattern shows two distinct cells in each hemisphere: in the tropics the Hadley cells, and in the mid-latitudes the Ferrel cells. The Hadley cells are characterized by a rising of warm, moist air in

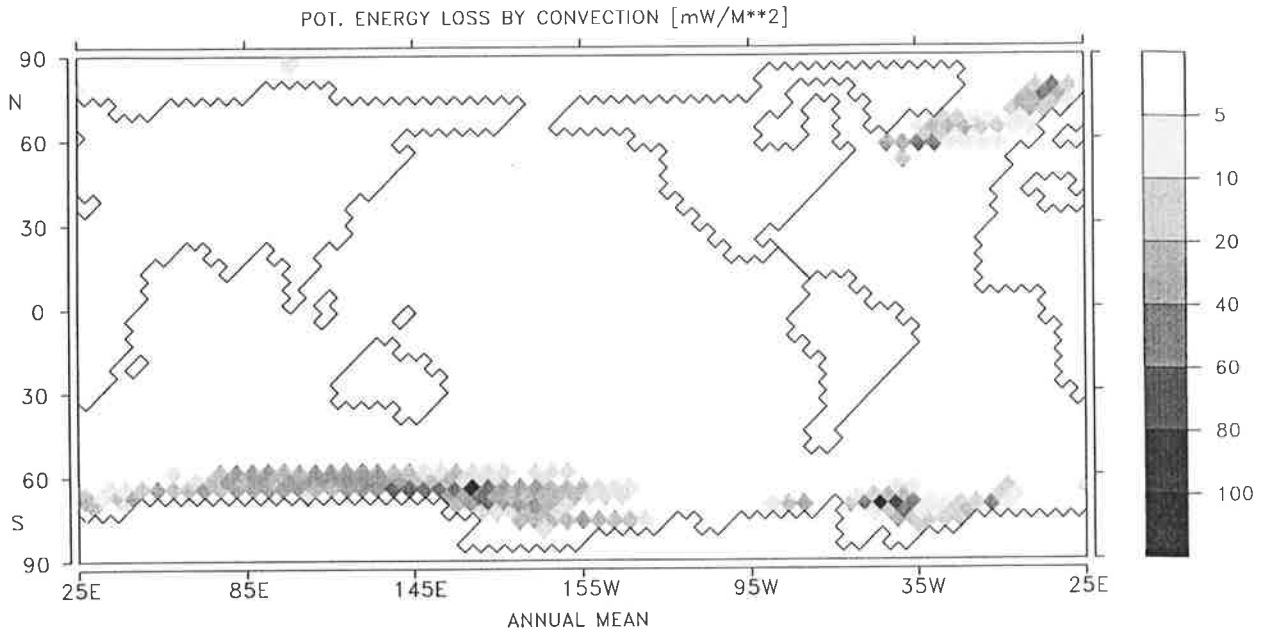

Figure 2: Loss of potential energy due to convection. Results are for final the decade (years 241-250) of control run (Exp. CTRL). The shown quantity gives an estimate of the efficiency of deep water formation in different locations.

the equatorial region and a sinking of colder air in the subtropics. In both model and observations the region of upward motion, the intertropical convergence zone (ITCZ), is centered on 5°N. The somewhat weaker thermodynamic indirect Ferrel cells are mainly produced by the cyclonic activity of the mid-latitudes. Compared to the ECMWF analysis, the Hadley cells of the model are too strong and the southern hemisphere Ferrel cell is too weak. Both features also appear in the uncoupled runs with our atmosphere model (cf. Roeckner et al., 1992).

Figure 4 compares the zonally averaged near-surface air temperature of the control run CTRL with observations from a climatological data set given by Legates and Willmott (1990). The seasonal means of December, January and February (DJF) and June, July and August (JJA) are plotted. The model near-surface air temperatures fit the observations reasonably well, with the exception of the polar latitudes in the southern hemisphere in JJA. The model temperatures are too warm, because the winter-ice cover is too small and the SSTs in this area are too warm. The global mean is slightly overestimated (by 0.6°C in DJF and by 0.9°C in JJA). Differences in the near-surface temperatures over land and sea depict a stronger land-sea temperature contrast in winter.

The net freshwater flux of the atmosphere model (precipitation minus evaporation) and of the ocean model (precipitation minus evaporation plus river runoff and flux correction) from experiment CTRL are shown in Figure 5. The flux correction was determined from the precipitation minus evaporation plus runoff field of the uncoupled AGCM, and the diagnostic freshwater fluxes were determined by relaxation to climatological sea-surface salinity (Levitus, 1982) in the OGCM. The rainfall maxima in the ITCZ and the high latitudes as well as the excess of evaporation in the subtropics are in qualitative accordance with each other and with estimates based on observations (Baumgartner and Reichel, 1975, Dorman and Bourke, 1981, Isemer and Hasse, 1987). The runoff of the major rivers to the oceans, such as the Yangtse,

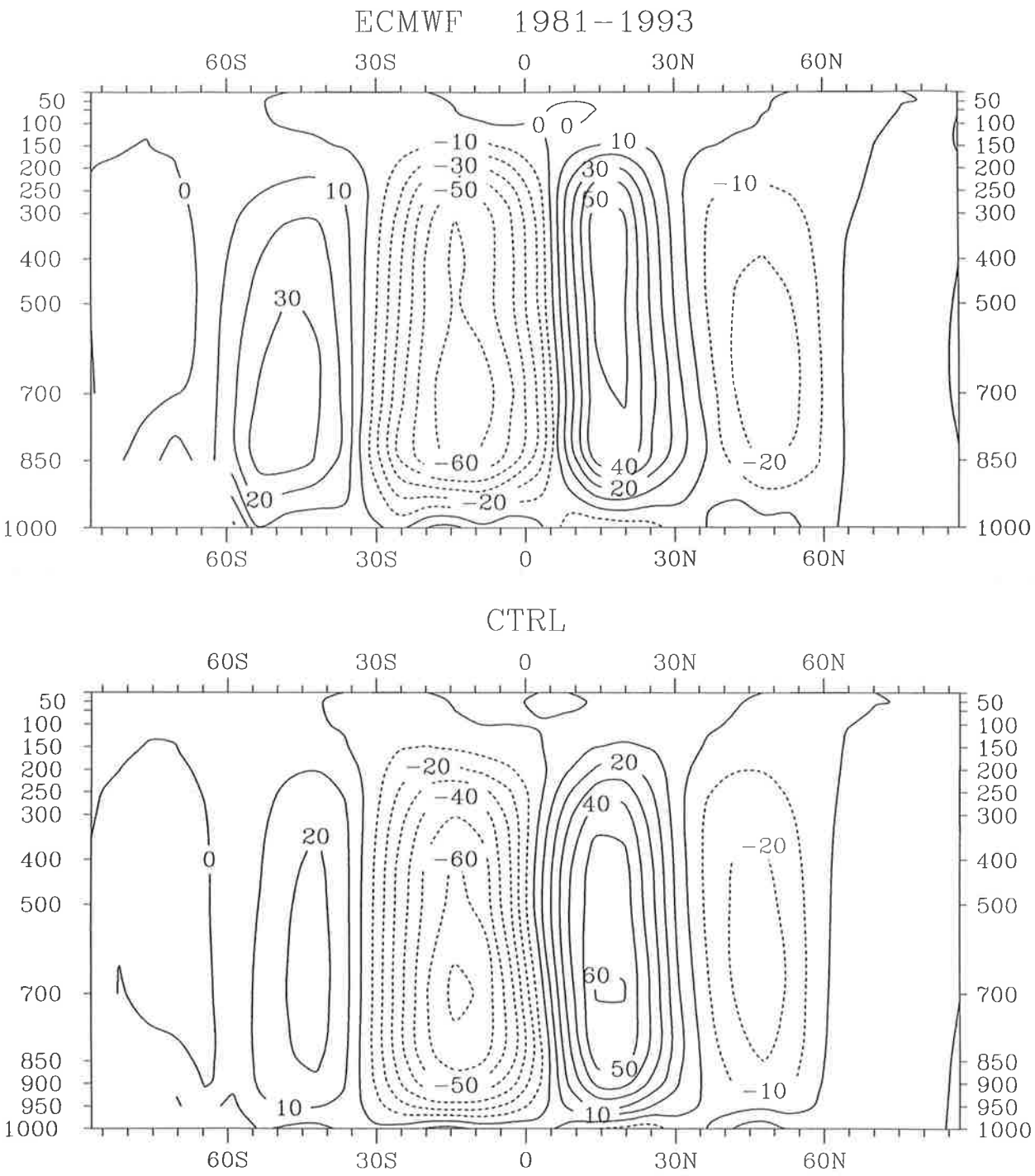

Figure 3: Zonal-mean cross section of the atmsopheric mass transport stream function. Fields for the ECMWF analysis of the years 1981 to 1993 (a) and for the final decade of the control run CTRL (years 241 to 250) (b). Positive values indicate clockwise rotation, contour interval is 10×10^9 kg/s.

Amazon and Congo, can be detected as local maxima in fig. 5b. Other features seem to be less realistic in the forcing field of the ocean, e.g. the dipole patterns close to the western boundary currents and strong positive freshwater fluxes close to the North Pole at 90°E and

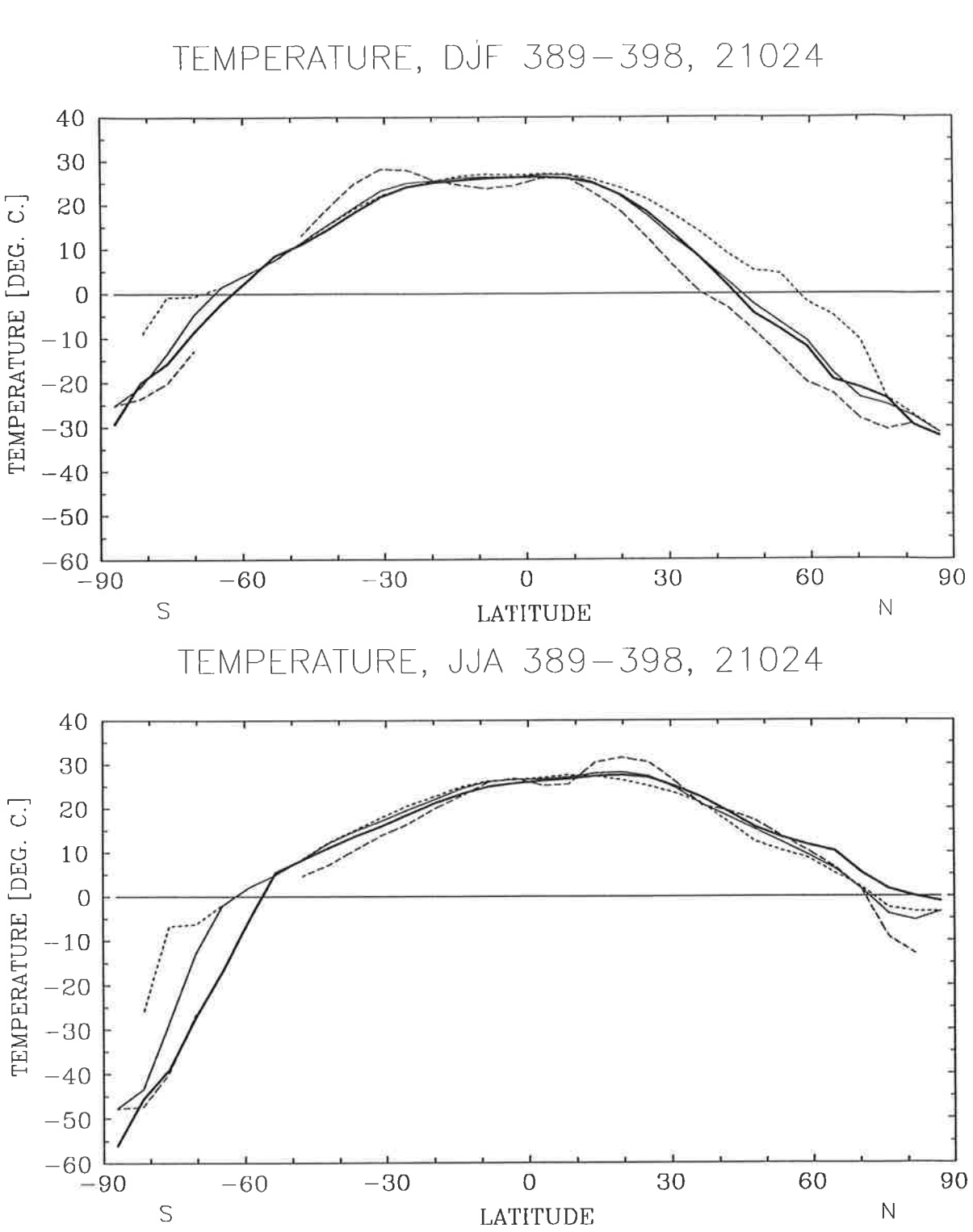

Figure 4: Zonally integrated mean surface temperature of winter season (a) and summer season (b). Thin solid line: total mean, dashed line: land, dotted line: ocean. Thick solid line: zonal mean of observations, based on the data set of Legates and Willmott (1990). Model results are for final decade (years 241-250) of control run (Exp. CTRL).

in the Southern Pacific. Integrated from the North Pole over the Atlantic (including the Arctic) to 30°S, the oceanic forcing field gives 0.35 Sv in the model; the Baumgartner and Reichel data give more than 0.5 Sv.

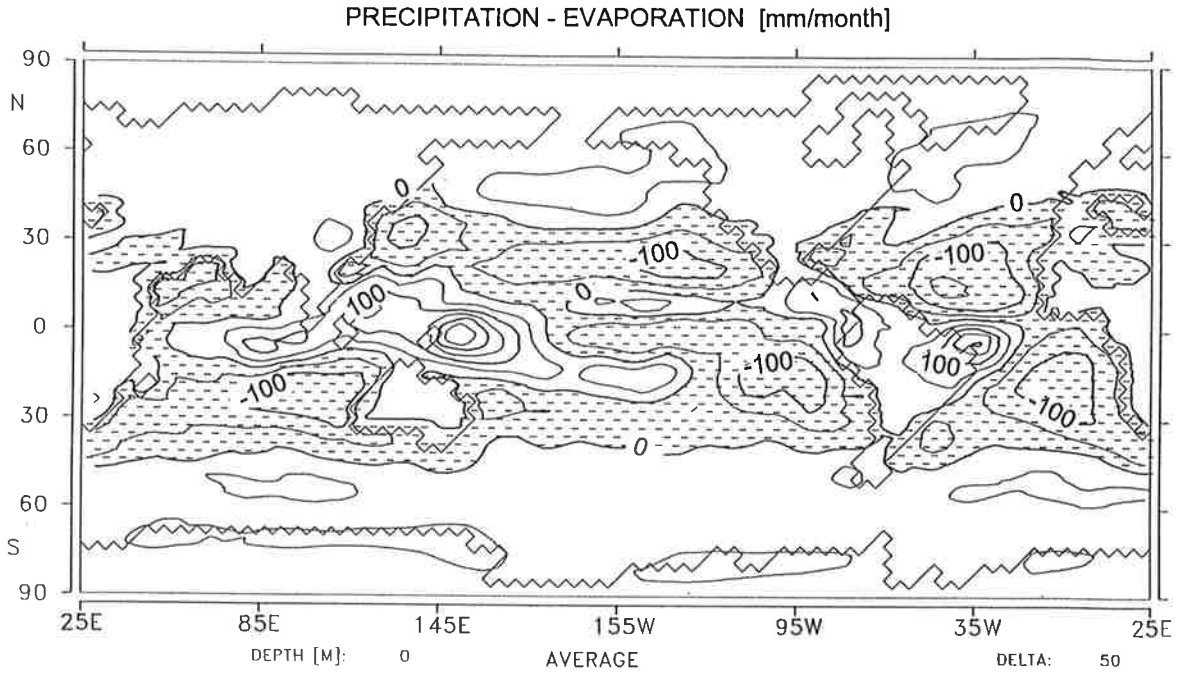

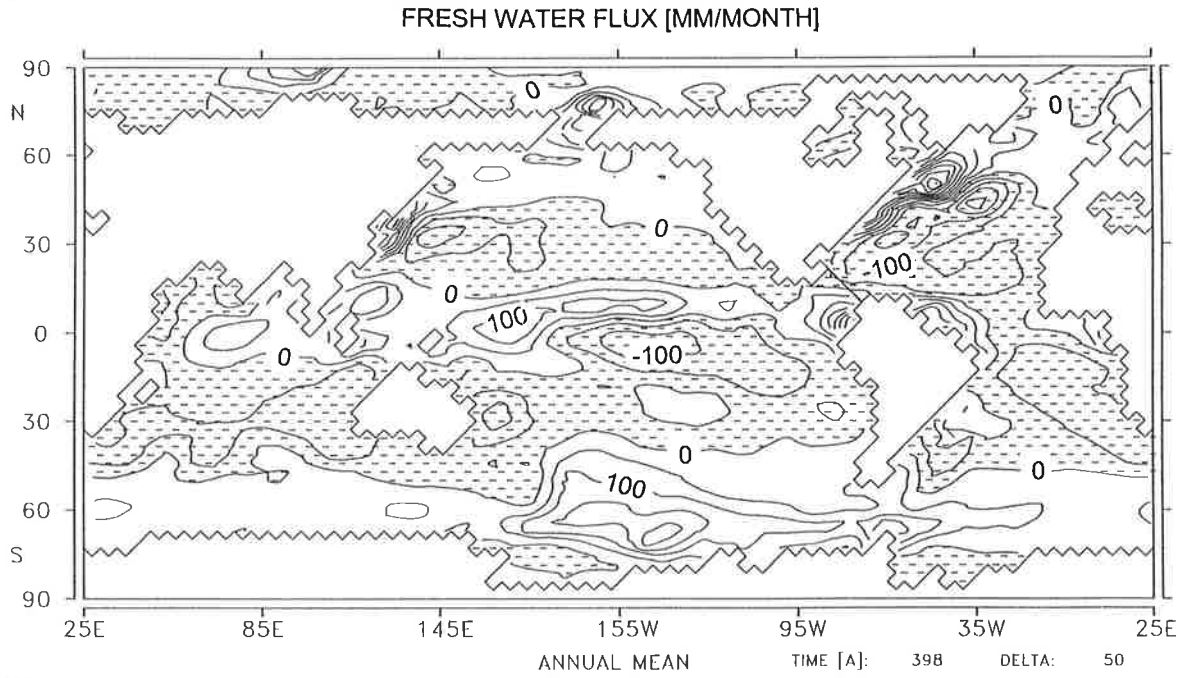

Figure 5: Annual mean net freshwater flux (a) of the atmosphere (precipitation minus evaporation) and (b) of the ocean (comprising precipitation minus evaporation, river runoff and flux correction), Exp. CTRL. C.I.: 50 mm/month. Results are for the final decade (years 241-250) of experiment.

3 Meltwater experiments

Figure 6 illustrates the sequences of several numerical experiments as a function of integration time and of additional meltwater input to the ocean. Subsections 3.1 and 3.2 describe meltwater experiments performed with the original model (schematic plot in Fig. 6a). Some

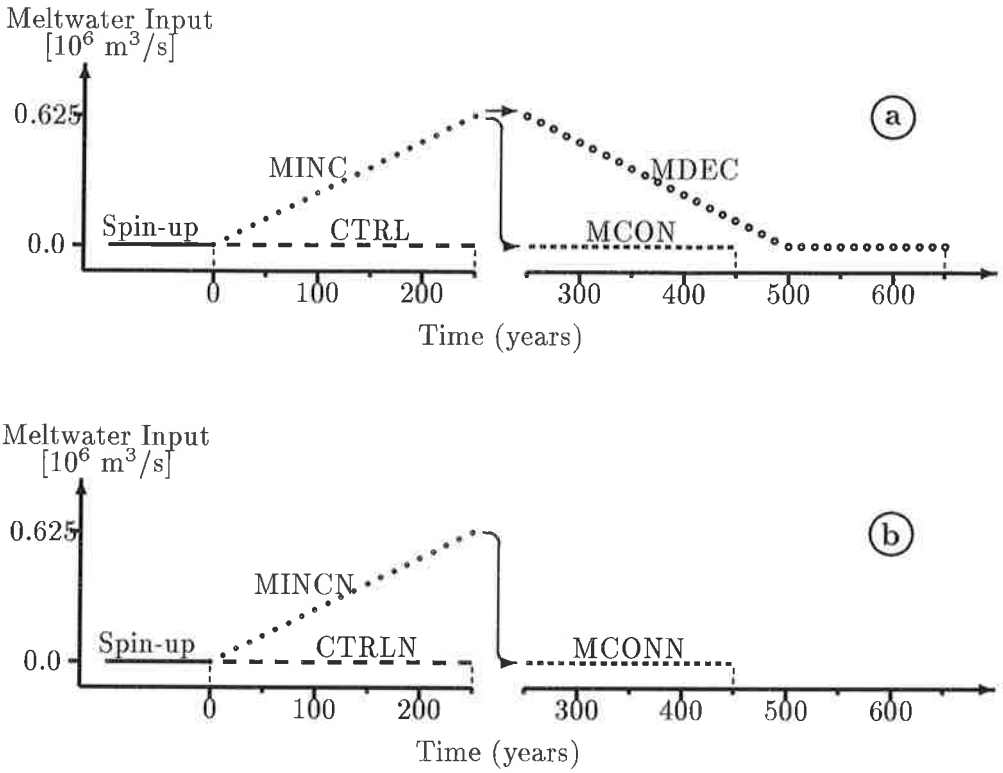

Figure 6: Notation of experiments as a function of integration time and additional meltwater input into the ocean. (a) with North Atlantic heatflux correction, (b) without North Atlantic heatflux correction. See text for further explanations.

of these experiments were repeated with a version of the model that omitted the heat flux correction in the North Atlantic. These experiments are denoted by an additional N at the end of their names. These experiments are represented schematically in figure 6b.

3.1 Experiment with increasing meltwater input

The coupled model was integrated over 250 years in time with a linearly increasing amount (0.0025 Sv/y) of meltwater discharge into the North Atlantic, ranging from zero up to 0.625 Sv (1 Sv $\equiv 10^6$ m^3/s) in the year 250 (Exp. MINC - Meltwater input INCreasing - in Fig. 6a). The meltwater was released in equal parts to two grid points on the Canadian coast of the Labrador Sea. As a consequence, the global mean net freshwater flux to the ocean was no longer balanced. The accumulation of the additional meltwater led to a rise in the global mean sea level of about 6.7 m at the end of experiment MINC. The location of the prescribed meltwater input is meant to be a highly idealized analogue of the melting of the Laurentide ice sheet. The location of the input is meant to resemble one of the potential sites of meltwater release to the Atlantic. The magnitude of the prescribed meltwater input is within the range derived from geological records, as Fairbanks (1989) gives a peak value of more than 0.45 Sv meltwater input averaged over several hundred years estimated from the time evolution of global mean sea level, which was derived from Barbados corals. The ramping up allows an

estimate of the hysteresis curve of the coupled ocean-atmosphere system and is similar to the experiment by MM94. The changes in forcing are probably too fast for the system to be close to quasi-equilibrium as in the experiments of MM94, but we had to compromise here to keep the experiments affordable.

This subsection describes the main differences between the final states of ocean and atmosphere, respectively, obtained with the control experiment CTRL and the meltwater release experiment MINC. The analysed quantities represent transient features averaged over the last decade of meltwater input from a short synchronous integration. Due to the strong perturbation (meltwater input of more than 0.6 Sv) the climate system in the model is definitely not in a steady state. Therefore, our results must be interpreted with more caution than those based on steady state solutions. However, as the fields of SST and sea-ice and the atmospheric circulation did not show any significant drift during these periods, we will assume that they are in a quasi-equilibrium with the slowly varying circulation of the deep ocean.

The time histories of several parameters characterizing the state of the ocean in the experiment with strong additional meltwater input (Exp. MINC) and in the control run (Exp. CTRL) are shown in Figure 7. The time series of the total freshwater input to the North Atlantic (i.e. the sum of freshwater flux plus additional meltwater discharge) is shown in Figure 7a. After about 100 years the total release of potential energy by convection (integrated over the North Atlantic north of 30°N and the Arctic), which is a good proxy of the actual formation rate of NADW, was notably weaker (Fig. 7b). The additional meltwater input slowed down the Atlantic thermohaline circulation. This led to a reduced poleward heat transport in the northern North Atlantic (including a regional drop in sea surface temperature, see Fig. 7f), and consequently the ice volume increased (Fig. 7c). After about 150 years the convection was almost totally suppressed. When the convection was reduced to about 50% of the control run, the meltwater input had a value of about 0.22 Sv. At the time of total suppression of NADW formation in year 150, the meltwater input had a value of 0.38 Sv. The threshhold values for constant input to suppress NADW formation must be expected to be somewhat lower due to the relatively fast changes in the prescribed meltwater forcing.

After shutdown of NADW formation, it took another fifty years for the atmosphere-ocean heat exchange and the volume of the North Atlantic sea-ice to reach new equilibrium values. At this time the sea-ice volume is five times as large as in the control run (110×10^{12} m^3) and the Atlantic heat transport has been reduced to about 0.1 PW. The response of the ocean in such quantities as heat transport and formation rate of NADW to the linear enhancement of meltwater input is rather smooth. This is contrary to the transition behaviour of our ocean model when run with traditional mixed boundary conditions (cf. MM89). In those experiments the thermohaline circulation showed a highly nonlinear response, in particular in the abrupt suppression of convection and the diminishing heat transfer from the ocean to the atmosphere. Our results support the arguments that traditional mixed boundary conditions are inappropriate for investigating the stability of the thermohaline circulation (e.g. MM94, or Rahmstorf and Willebrand 1995).

Due to strong convection in experiment CTRL, the North Atlantic lost a large amount of heat to the atmosphere (0.7×10^{15} W in Fig. 7d). In contrast, in experiment MINC the reduced northward advection of warmer water masses and the increasing sea-ice coverage led to much less oceanic heat being released to the atmosphere. In the first 50 years of the experiment MINC the deep meridional circulation of the Atlantic was only slightly affected by the increasing meltwater release (Fig. 7e). As a consequence of the reduced convection in

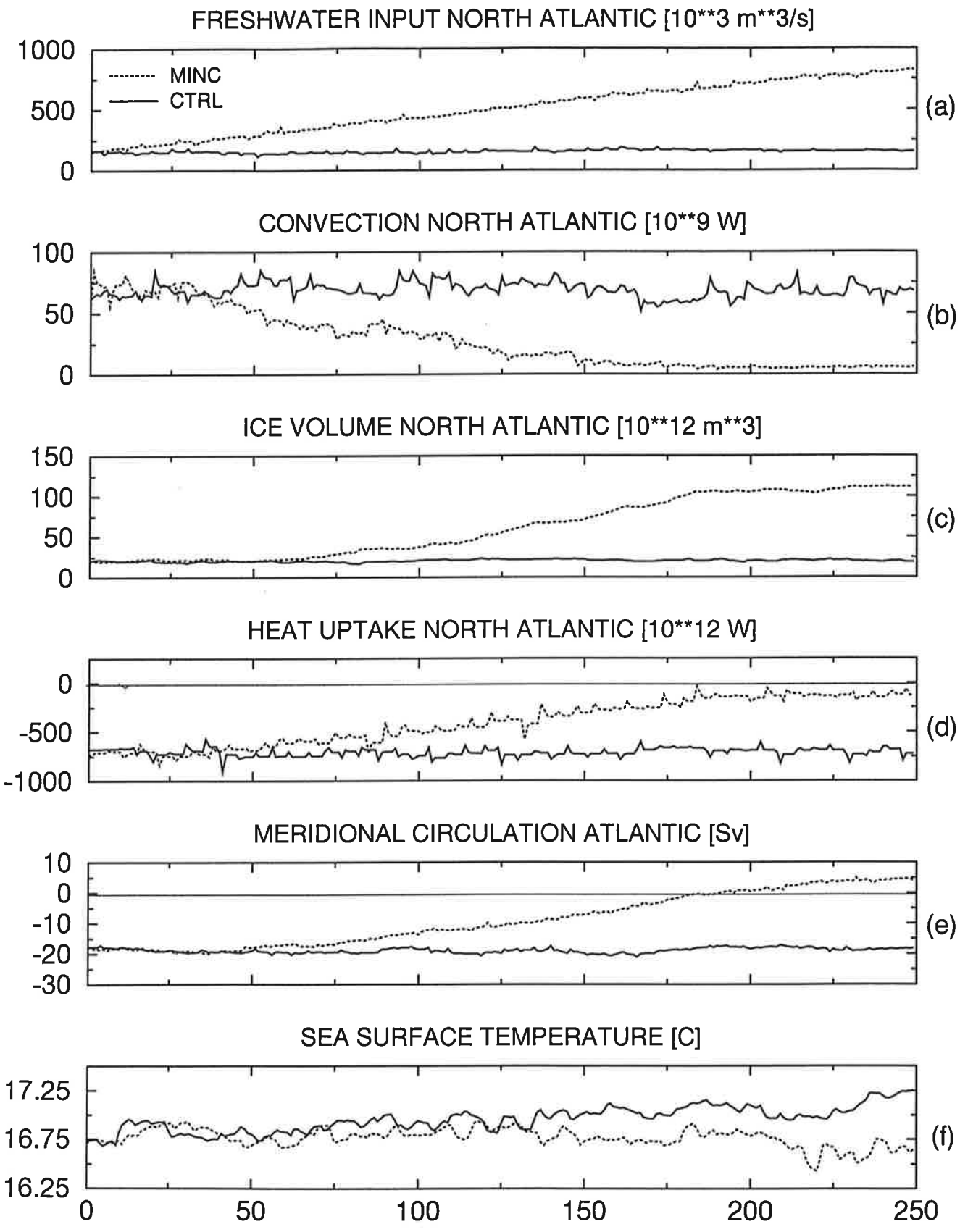
FRESHWATER INPUT NORTH ATLANTIC [10**3 m**3/s]
1000
500
0
MINC
CTRL
(a)
CONVECTION NORTH ATLANTIC [10**9 W]
100
50
0
(b)
ICE VOLUME NORTH ATLANTIC [10**12 m**3]
150
100
50
0
(c)
HEAT UPTAKE NORTH ATLANTIC [10**12 W]
0
-500
-1000
(d)
MERIDIONAL CIRCULATION ATLANTIC [Sv]
10
0
-10
-20
-30
(e)
SEA SURFACE TEMPERATURE [C]
17.25
16.75
16.25
(f)
0
50
100
150
200
250

Figure 7: (previous page) Time series (in years) of (a) prescribed meltwater plus freshwater input into the North Atlantic north of 30°N , (b) potential energy release through convection in the North Atlantic, (c) ice volume of the North Atlantic, and (d) heat uptake of the North Atlantic. (e) Northward transport at 30°S in the Atlantic below 1500 m. (f) Globally averaged sea surface temperature. Notation of experiments is given in upper left corner of (a). All data are annual means without further filtering.

the North Atlantic, however, the amount of southward-flowing NADW at 30°S below 1500 m gradually began to cease. This depth corresponds to the minimum of the overturning streamfunction, thus indicating of the total outflow of NADW. After about 200 years the direction of the deep water transport changed sign, and below 1500 m about 5 Sv of northward flowing AABW were found. The circulation pattern changed drastically and the extreme value of the overturning stream function was no longer found at 1500 m but at 2500 m. The maximum of this cell had a strength of 9 Sv.

The globally averaged sea surface temperature (SST) of experiment MINC (Fig. 7f) decreases about 0.5°C during the integration period relative to the control run (Exp. CTRL). Except for the last fifty years, the temperature of the meltwater experiment seems to be remarkably constant during the experiments. Nevertheless, the control run shows a notable climatic drift of the coupled ocean-atmosphere system of about 0.4°C during 250 years, which resulted in the relative cooling of experiment MINC.

3.1.1 Changes in ocean circulation

The large meltwater release reduces the near-surface salinity in experiment MINC in the whole Atlantic and produces a freshwater cap over the high-latitude North Atlantic (Fig. 8). Near the sites of the meltwater input, the near-surface salinities are as low as 25 psu. Except for the Arctic and the Atlantic, the salinity differences in other ocean basins are comparably small. There is, however, a salinity decrease of about 1 psu in the Northwest Pacific (not shown).

The strong salinity differences lead to relatively low North Atlantic surface densities in experiment MINC (not shown), as the effect of temperature changes on density is relatively small for low temperatures. As a consequence, the stability of the stratification increases and deep convection in the North Atlantic and thus NADW formation are totally suppressed (see Fig. 7b). The suppression of NADW-formation leads after 50 years to a reversal of the thermohaline circulation (see Fig. 9). The strong conveyor belt cell of NADW, which was present in the control run (see Fig. 1), is now completely wiped out. Instead the Atlantic is now ventilated from the Southern Ocean with AABW. This shows up as an intensification of the AABW cell by 15% at the end of experiment MINC and a much larger extent of this cell. However, as noted before, this circulation pattern is not in a steady state, but corresponds rather to a transitional behaviour. The overall convection in the Southern Ocean and thus the total formation rate of AABW are not significantly affected by the meltwater input.

The reduced flow of surface water into the Atlantic as part of the conveyor belt circulation also leads to strong changes the surface velocity field. The most pronounced differences are in the Atlantic (Fig. 10a,b). In experiment CTRL the main Gulf Stream flow penetrates northward until it reaches the GIN-Sea. This path is completely interrupted in experiment MINC. Instead, a weak Gulf Stream separates further south of the American coast and extends only

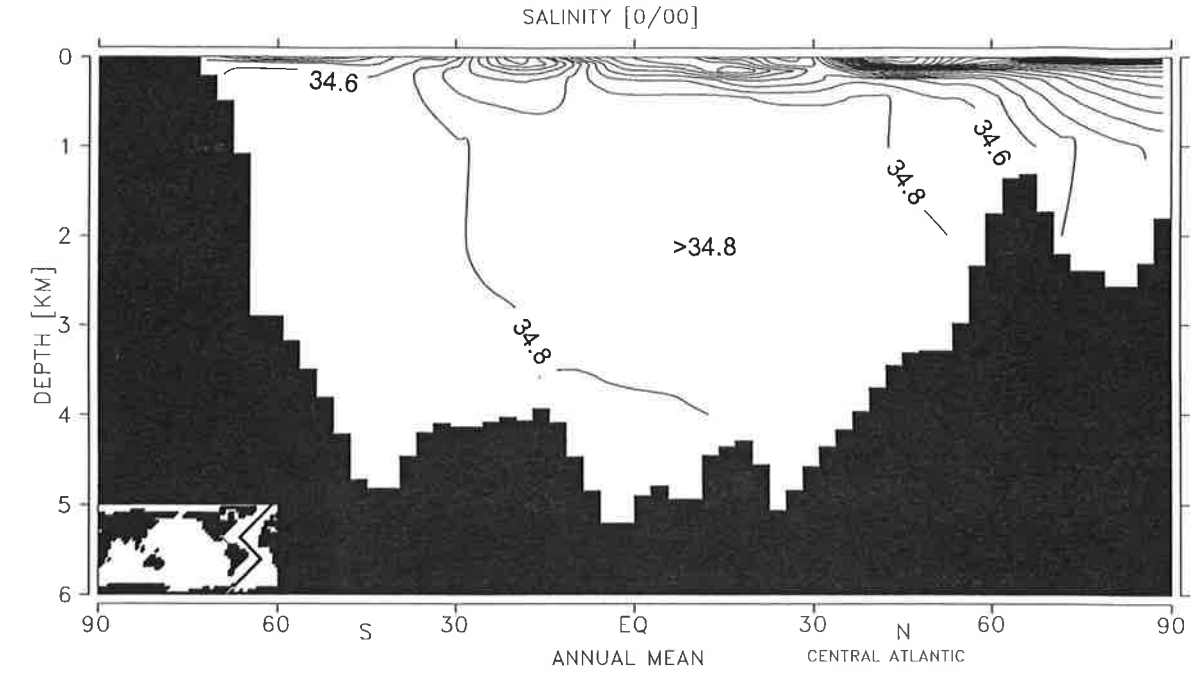

Figure 8: Salinity section in the central Atlantic of Exp. MINC. C.I.: 0.2 psu. Results are for the final decade (years 241-250) of experiments.

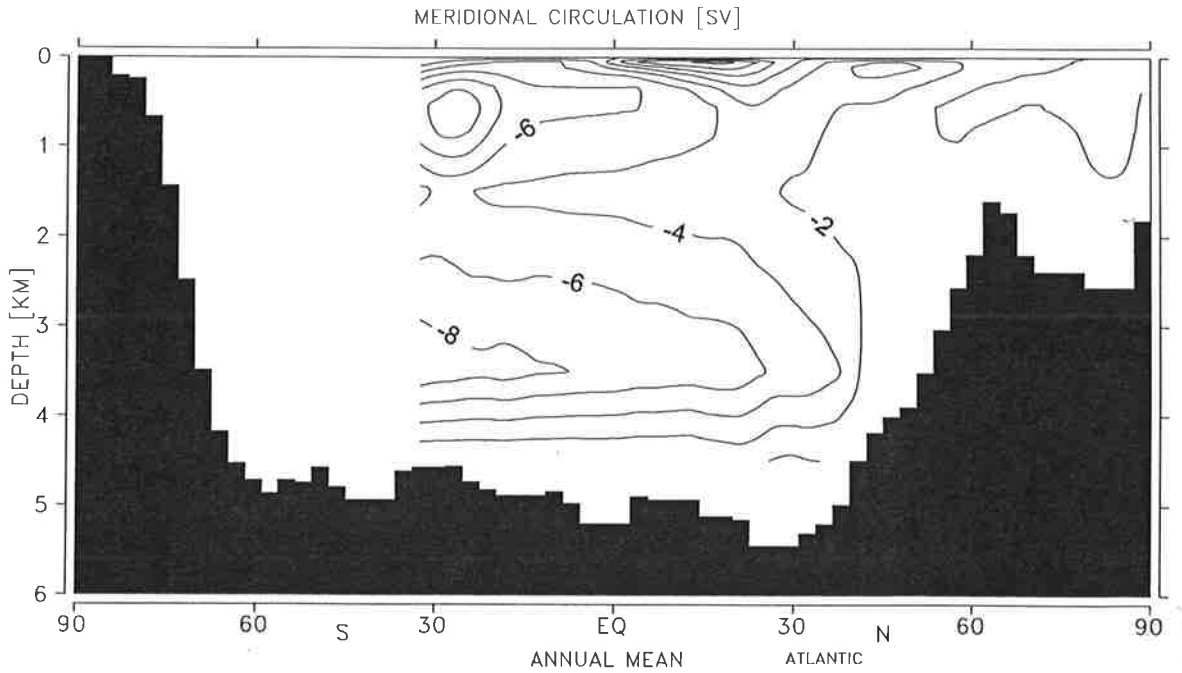

Figure 9: Zonally integrated meridional mass-transport streamfunction of the Atlantic. Results are for the final decade (years 241-250) of Exp. MINC. Positive values denote clockwise rotation. C.I.: 2×10^6 m^3/s.

to an area south of about 40°N (Fig. 10a). An intensified East Greenland Current supplies the water that flows southward along the European west coast as an intensified Canary Current, finally constituting the strengthened North Equatorial Current. Even the equatorial currents are considerably weakened in experiment MINC. The Brazil Current is significantly stronger than in the control run. Another important feature of the flow is the reversal of the transport through the Bering Strait. In the subtropical South Atlantic the northwestward velocity component has been reduced, indicating less inflow of surface water from the Southern Ocean. Arctic surface water, which has been further freshened through dilution with meltwater, flowing into the Pacific is responsible for the negative salinity anomaly in the Northwest Pacific.

The surface circulation pattern in the control run (Fig. 10b) advects warm and salty low-latitude water to the formation sites of NADW. The interaction with the atmosphere leads to a significant heat loss to the atmosphere. Additionally, the water becomes fresher once it enters the areas where precipitation is higher than evaporation (approximately north of 45°N). Due to the strong atmosphere-ocean interaction, the heat loss dominates and thus the surface density increases. Finally the density is high enough for NADW to form. The newly formed NADW flows southward at depths of 2 to 3 km. The northward transport in the upper layers is partly a compensation current for the deep outflow. The deep outflow therefore creates necessary conditions for its own existence, by forcing the northward advection of salty surface water, which in turn is a necessary condition for the formation of NADW and thus the deep outflow.

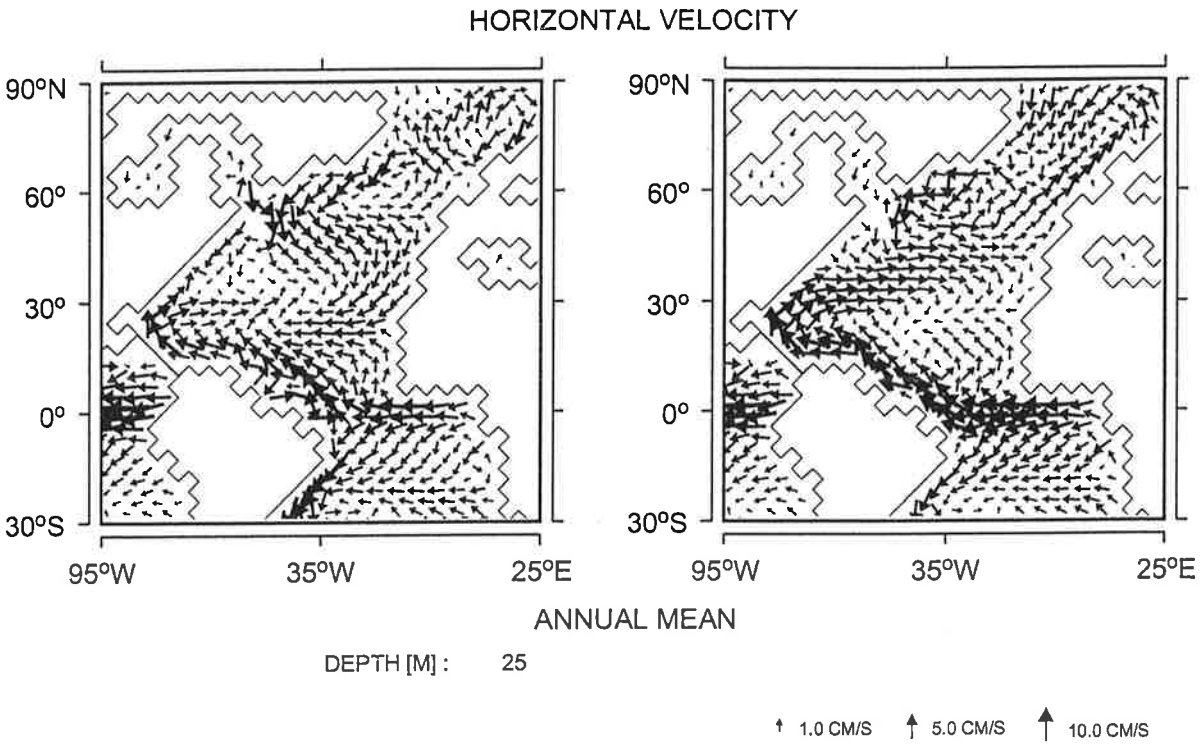

Figure 10: Surface currents in the Atlantic sector of the model. Results are for the final decade of Exp. MINC (a) and Exp. CTRL (b). See lower right corner for scaling of velocity vectors.

In the meltwater experiment MINC this selfstabilizing chain of processes is interrupted. There is no longer a northward surface transport of salty water into the polar regions of the Atlantic. This means the surface water in polar and subpolar regions is exposed longer to the net precipitation at high latitudes, which dilutes the surface salinity even further. This effect amplifies the effect of the added meltwater, as there is no relevant direct feedback of the surface salinity on the atmospheric freshwater fluxes. This advection effect alone can be sufficiently strong to permit the existence of multiple steady states of the thermohaline circulation. The positive advective feedback for the thermohaline circulation is well known and has been studied in many models of widely different complexities (e.g. Stommel, 1961, for box models, Bryan, 1986, for OGCM, and MS88 for coupled OAGCMs).

3.1.2 Changes in surface temperature

The strong changes in the ocean's surface circulation, thermohaline-driven overturning and associated heat transport show up as marked changes in SST and sea-ice cover (Fig. 11). The SSTs of the whole North Atlantic are colder than in the control run CTRL (over 8.5°C in the annual mean around Iceland and in the Norwegian Sea, Fig. 11b). Consequently, the maximum in sea-ice extent now touches the American coast south of Newfoundland and even covers parts of the coasts of the British Isles. The Norwegian Sea is completely ice-covered.

In the experiment CTRL the relatively warm climate of the North Atlantic (compared to other places on the same latitude belt) is caused by advection of warm low-latitude surface water in the upper branch of the conveyor belt circulation. Once this overturning circulation has been interrupted, the Atlantic northward heat transport at 30°N is reduced from 0.7 PW to 0.1 PW. With the reduced northward oceanic heat transport, the SST drops to the freezing point and sea-ice forms, isolating the ocean surface from the atmosphere. Due to the increased stability, no deep mixed layer can form in winter and thus the effective heat capacity of the mixed layer is reduced significantly, leading to an even stronger cooling in winter. Whereas the heat fluxes from the ocean to the atmosphere due to physical processes essentially vanish when the sea-ice is thick, the heat flux correction continues to extract heat from the ocean in some areas. This leads to the artificial development of very thick sea-ice in the GIN-Sea. It will be shown below that this artefact of the model does not effect the results regarding the stability of the thermohaline circulation (see section 3.3).

The differences in near-surface air temperature between the experiments MINC and CTRL for the annual mean and northern winter season, respectively, are illustrated in Figures 12a,b. The difference pattern looks quite similar to those of SST, although the annual mean difference in near-surface air temperature (more than 20°C in the northern North Atlantic) exceeds by far the difference in SST (Fig. 11b). This signal is even more amplified in the northern hemisphere winter (Fig. 12b), where the atmospheric temperature differences exceed 33°C. This can be explained by the small solar irradiation in winter and the southward extension of the sea-ice cover. The latter effectively isolates the atmosphere from the surface ocean (and its heat capacity). Additionally, the cloud cover in winter is reduced north of 60°N, which makes the wintertime cooling by longwave radiation more efficient.

The belt of maximum differences in near-surface air temperature is shifted to further north than the corresponding belt for SST. This effect is amplified in winter, where the maximum difference in near-surface air temperature is around 70°N, whereas the maximum in SST difference is around 60°N. The reason for this difference is the intensified spreading of sea-ice in experiment MINC, which results in larger changes in near-surface air temperature

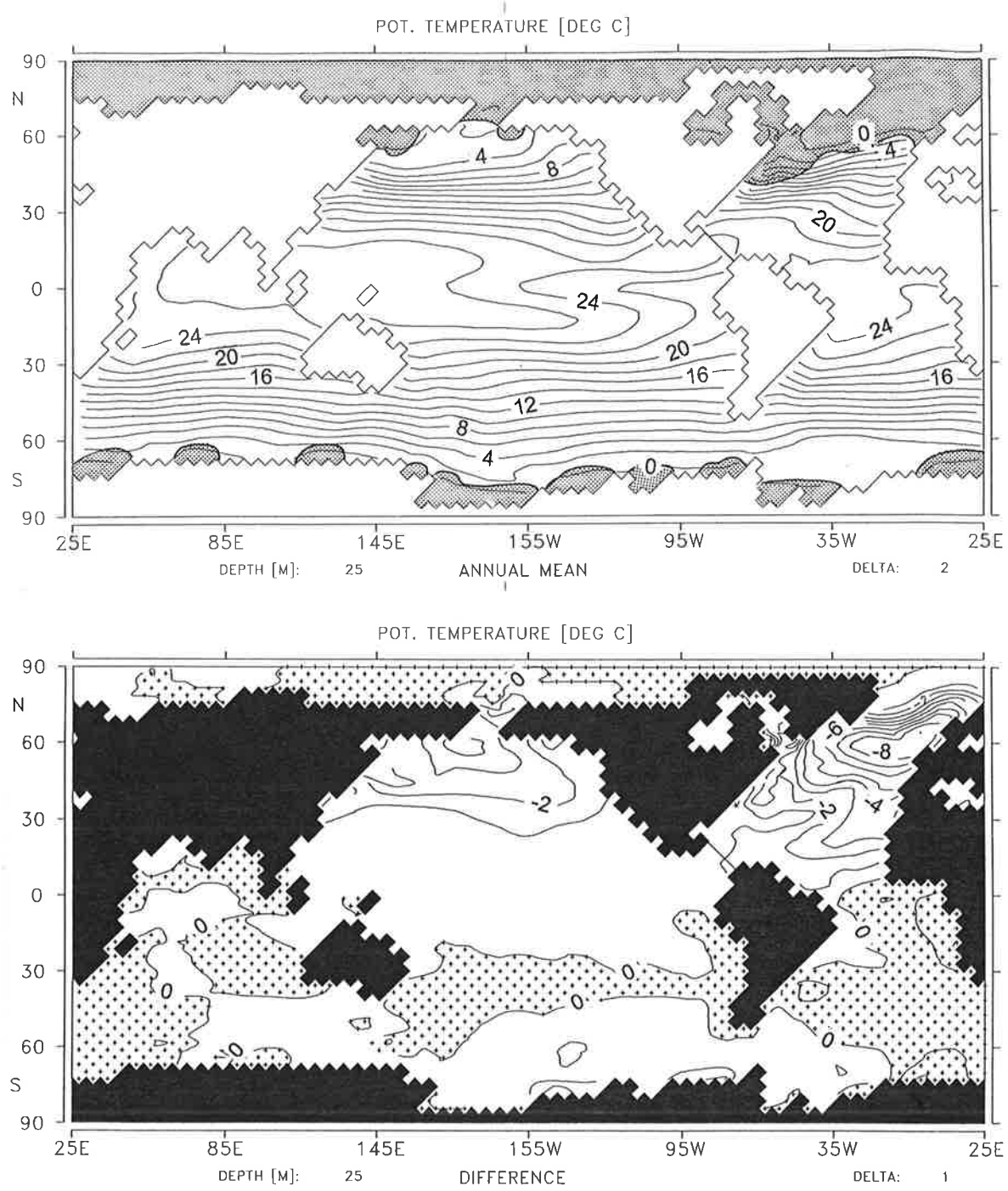

Figure 11: (a) Annual mean sea-surface temperature (SST) of Exp. MINC. Shaded area denotes the maximum in sea-ice extension. C.I.: 2°C. (b) SST difference between experiments MINC and CTRL, shading indicates positive values. C.I.: 1.0°C. Results are for the final decade (years 241-250) of experiments.

than in SST. In contrast to the air temperature, the cooling in the SST is limited by the freezing point of sea water.

In the North Pacific region both SST and near-surface air temperatures are considerably colder in experiment MINC than in the control run CTRL. Although the anomalies are much smaller in amplitude with slightly more than 4°C in SST (see Fig. 11b), they are of climatic importance. Whereas the cooling in the North Atlantic can be found in all oceans only

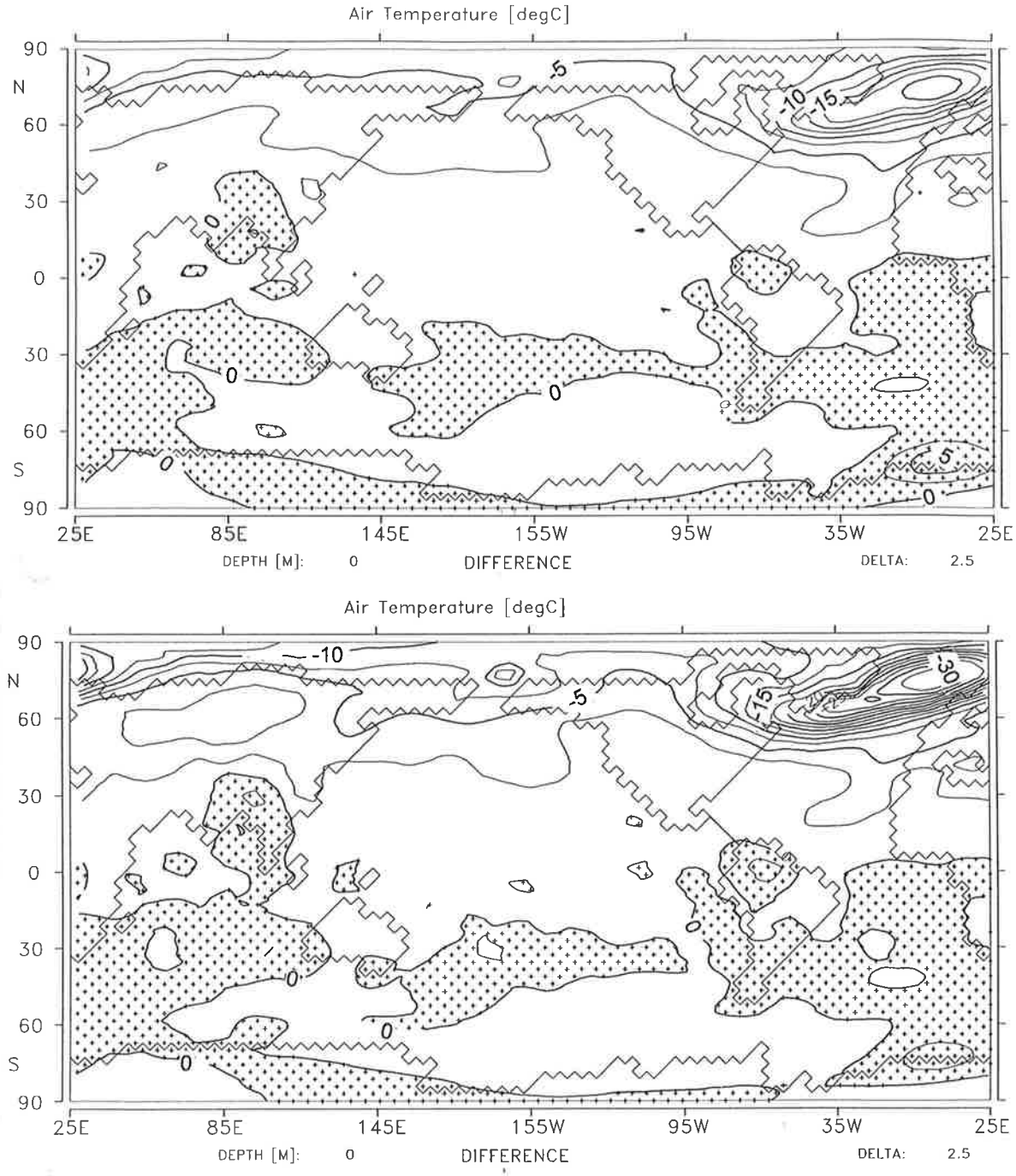

Figure 12: Difference in near-surface air temperature between the experiments MINC and CTRL. (a) Annual mean values, (b) northern winter season (DJF). C.I.: 2.5°C, shading denotes positive values. Results are for the final decade (years 241-250) of experiments.

GCM simulations (e.g. MM89, Marotzke and Willebrand, 1991, Weaver and Sarachik, 1991, MM94, Rahmstorf and Willebrand, 1995), the cooling in the Pacific is generally missing. It has only been found in the coupled OAGCM of MS88, who suggested that the cooling in the North Pacific may be caused by zonal advection of Atlantic thermal anomalies through the atmospheric circulation. Due to the processes of advection and diffusion, the cooling extends over the entire extratropics of the northern hemiphere. Off the African coast in the South Atlantic a positive SST anomaly of more than 1°C is a consequence of the reduction of inflow

of cold surface waters from the Southern Ocean. The small positive anomaly off Argentine is due to a southward shift of the water-mass boundary between Subtropical Atlantic water and the ACC. The moderate temperature changes along the Antarctic continent are related to regional shifts in sea-ice cover and convection patterns, whereas for the rest of the southern hemisphere the temperature is almost unchanged.

The changes in SST also have a dynamical effect on the ocean circulation. The strong cooling in the North Atlantic SSTs tends to cancel out at least part of the effect of the reduced salinities on surface density (freshening lowers surface density; cooling increases it). By reducing the density anomaly, the cooling also reduces the circulation anomalies created by salinity anomalies. This reduces the strength of the positive feedback process on high-latitude negative salinity anomalies through changes in the residence time at the surface. During the final phase of very high meltwater release, the densities are clearly determined by the salinities. However, the temperature effect is important in earlier phases of the experiment, as is determines the strength of the net feedback acting on the negative salinity anomalies and thus determins the stability of the conveyor belt circulation, as was demonstrated in OGCMs by varying the upper boundary condition for temperature (Zhang et al., 1994, MM94, Rahmstorf and Willebrand, 1995). Thus the surface cooling due to the suppressed oceanic heat advection is a feedback stabilizing the present mode of the thermohaline circulation.

3.1.3 Changes in atmospheric circulation

The strong changes in SST and sea-ice distribution in the meltwater experiment MINC have a strong impact on the atmospheric circulation as well. The cooling at high latitudes of the northern hemisphere is not restricted to the surface but extends vertically over the entire troposphere, decreasing with height (not shown). As a consequence, the general circulation of the northern hemisphere exhibits considerable differences to the control run.

Figure 13 compares the geopotential height fields of the northern hemisphere at 500 hPa of experiments MINC and CTRL for both winter (DJF) and annual mean. In the control run (CTRL) the structure of the geopotential height field is very similar to the fields simulated by the uncoupled ECHAM3 simulations (cf. Roeckner et al., 1992). Compared to observations, both models underestimate the North Atlantic trough. The largest differences between the experiments MINC and CTRL are found east of Greenland, where negative anomalies of more than 22 gpdm in winter occur. This means that in the meltwater experiment the trough to the west of Greenland has a larger extension to the east and the flow over the North Atlantic becomes more zonal. In the Atlantic sector, the stronger meridional gradient of the geopotential height field (caused by the intensified north-south temperature gradient) leads to stronger westerly winds. A similar, but weaker, tendency can be seen over the North Pacific.

The pattern of the differences in summer is very similar to the winter pattern. In accordance with the much smaller temperature response in the meltwater experiment, the amplitude of the pattern is almost halved (not shown). Consequently, the annual mean geopotential height fields exhibit smaller deviations than the corresponding winter fields. The maximum change in the annual mean field is only 16 gpdm.

The changes in SST and sea-ice distribution not only affect the mean state of the atmospheric circulation but also its variability. For experiments MINC and CTRL the 500 hPa geopotential height fields of the winter season (DJF) were bandpass-filtered with a temporal window of 2.5 to 6 days (Blackmon, 1976). This time range is typical for variability generated by cyclones, so the standard deviation computed from these data is a good indicator of

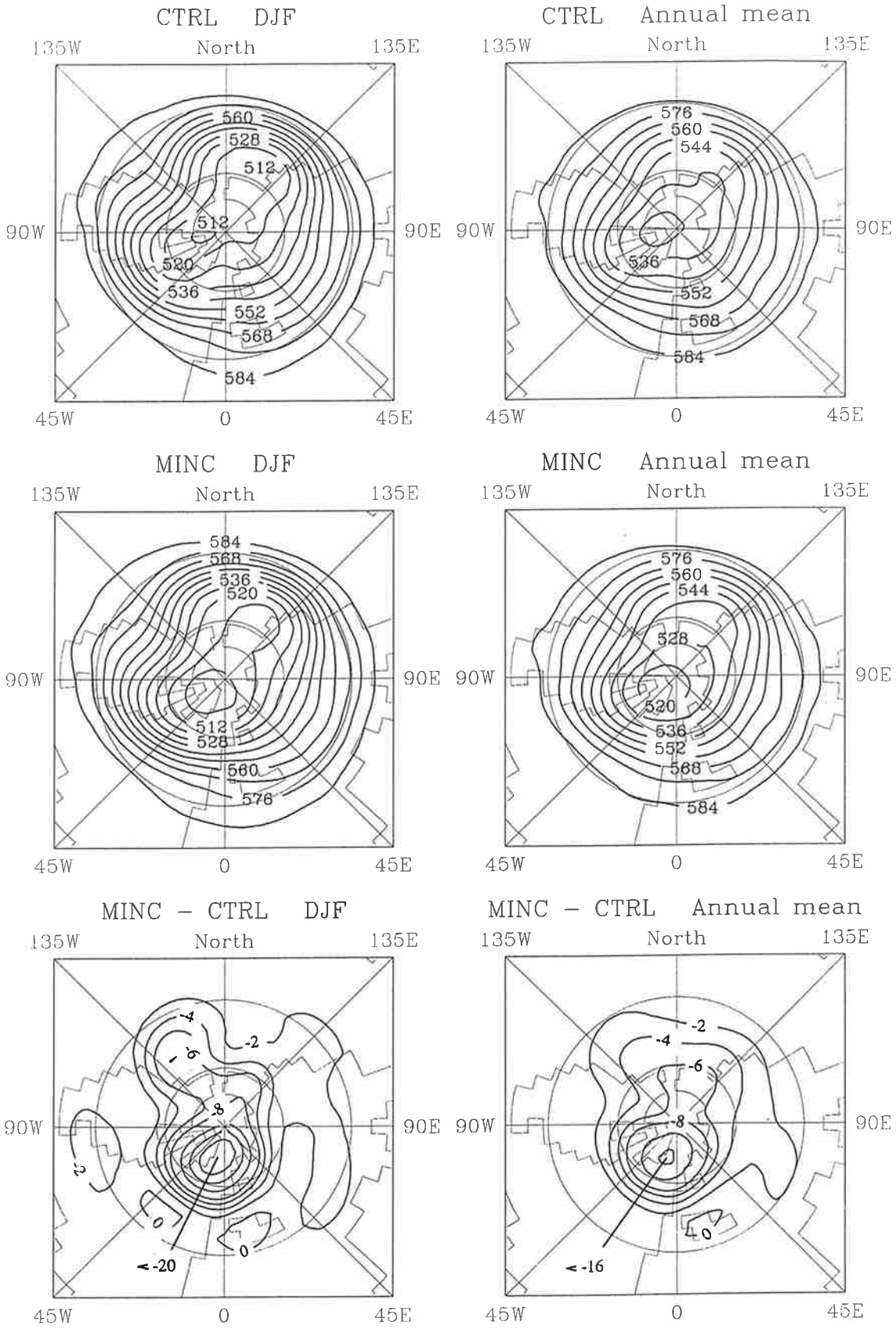
CTRL DJF
135W
North
135E
90W
90E
45W
0
45E
560
528
512
512
520
536
552
568
584
CTRL Annual mean
576
560
544
536
552
568
584
MINC DJF
584
568
536
520
512
528
560
576
MINC Annual mean
576
560
544
528
520
536
552
568
584
MINC – CTRL DJF
-4
-2
-6
-8
-2
0
0
< -20
MINC – CTRL Annual mean
-2
-4
-6
-8
0
< -16

Figure 13: (previous page) Geopotential height of 500 hPa for the experiments CTRL and MINC. Panels show results for DJF (left column) and annual mean (right column) of experiments CTRL (top), MINC (middle) and their difference. Contour interval for the climates is 8 gpdm, and variable (2, 5, 10, 15, 20 gpdm) for the differences maps.

cyclone activity. The distributions for DJF in the northern hemisphere for experiments CTRL and MINC are shown in Fig. 14. In both experiments the strongest variability can be found over the North Pacific and North Atlantic. In the meltwater experiment, MINC, the variability is greater than in the control run and the maxima are extended further to the east. As a result, the western parts of North America and Europe especially are affected by higher cyclone activity.

The changes in SST and sea-ice distribution not only affect the atmospheric circulation in the northern hemisphere extratropics, but also the tropical circulation. This can be seen in the zonal-mean cross-section of the atmospheric mass-transport stream function (Fig. 15, cf. Fig. 3). In the meltwater experiment, MINC, the vanishing crossequatorial heat transport in the Atlantic leads to a stronger Hadley cell in the northern hemisphere, whereas the southern hemisphere Hadley cell is slightly weakened. The intensification of the northern hemisphere Hadley cell is connected with an extension to the south. The ITCZ in experiment MINC is therefore centered (at least in the zonal mean) at the equator; the control run has a marked north-south asymmetry. Again, the response is strongest over the Atlantic.

Except for the equatorial regions and the North Atlantic and North Pacific the changes of wind-stress pattern are confined to coastal areas and do not have a marked impact on the global circulation. Figure 16 depicts the annual mean wind-stress field of experiments MINC and CTRL. In the meltwater experiment, the main difference from the control run

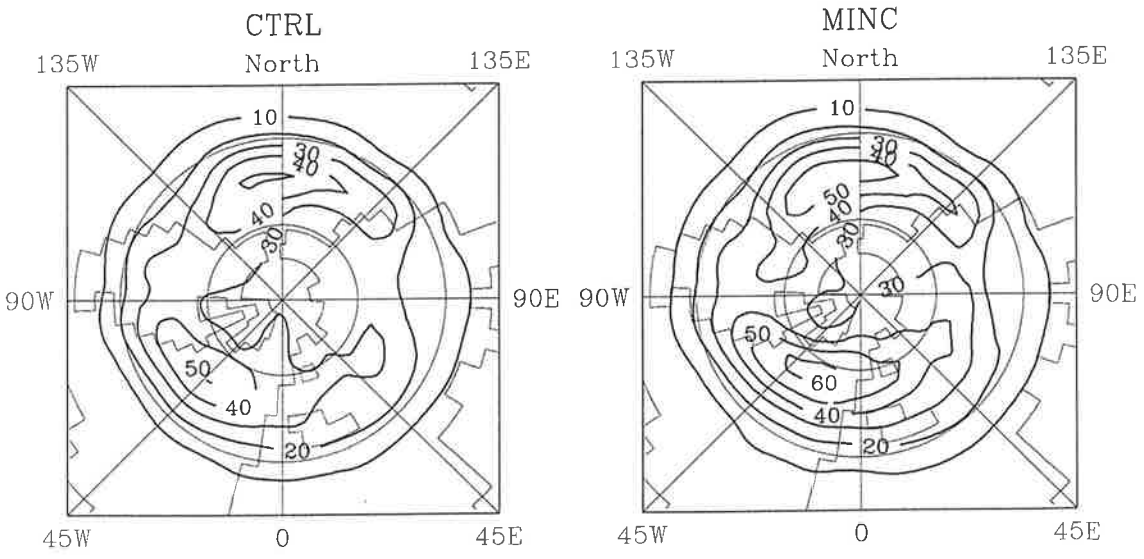

Figure 14: Standard deviation of bandpass filtered (2.5 to 6 days) 500 hPa geopotential height for DJF. Results are for the final decade (years 241-250) of (a) Exp. CTRL and (b) Exp. MINC. Contour interval: 10 gpm.

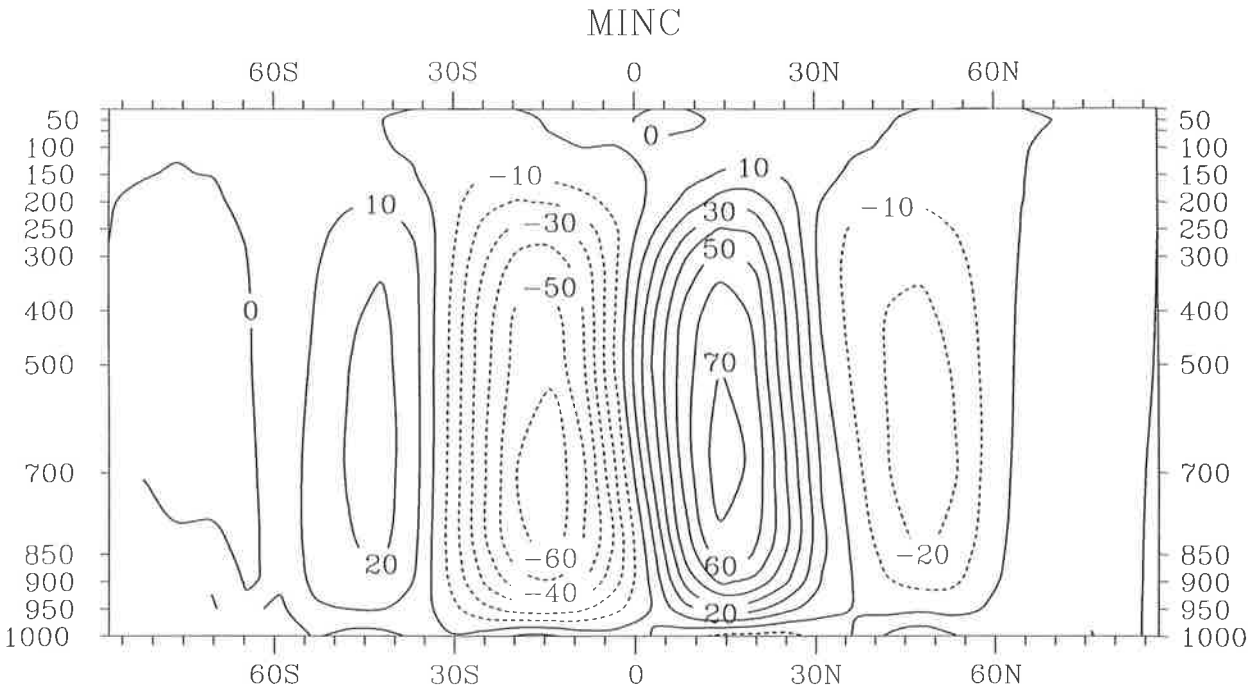

Figure 15: Zonal mean cross section of the atmospheric mass transport stream function for experiment MINC. Positive values indicate clockwise rotation, contour interval is 10×10^9 kg/s.

are the intensified westerlies around 50°N. The relative strength of the trade winds over the Atlantic (stronger in the northern, slightly weaker in the southern hemisphere) has also been modified. All these changes in the wind-stress pattern are closely related to the changes in the atmospheric circulation (Fig. 13) and thus to the enhanced meridional temperature gradients (Fig. 12). In addition to what one might expect from the thermal wind relationship, experiment MINC shows not only an increase of the wind-stress field along the west wind drift over the eastern part of the North Atlantic but also intensified wind stresses along the eastern coast of Greenland (southward) and the coast of Europe (northeastward). The amplitude of the cyclonic circulation over the Norwegian Sea in experiment MINC is significantly stronger than in the control run CTRL. This leads to augmented upwelling into the oceanic surface layer through intensified negative Ekman-pumping (i.e. Ekman-suction): $w_e = (\rho)^{-1} \nabla \times (\tau/f)$. It is especially the component $\partial\tau_y/\partial x$ of the wind-stress curl that contributes to the enhanced upwelling in the GIN-Sea. The effect of this modified vertical velocity in the ocean on the global circulation will be investigated in detail below.

Figure 17a illustrates the change in vertical velocity below the uppermost level averaged over the final decade of experiment MINC in the North Atlantic compared to run CTRL. This quantity is largely determined by Ekman pumping/suction. Over the entire GIN-Sea a stronger upwelling of typically 0.5 to 1 $10^{-6} m/s$ can be seen with an intensification towards the coasts. This anomaly leads to a weak but broad area of positive vertical velocity from the North American coast up to northern Europe in experiment MINC. The increased upwelling has a strong effect on the local stability. The overlying fresh surface water is moved away from the Norwegian Sea and saltier water from below is brought in contact with the surface. The export of fresh surface waters out of the GIN-Sea into the northern North Atlantic by the East

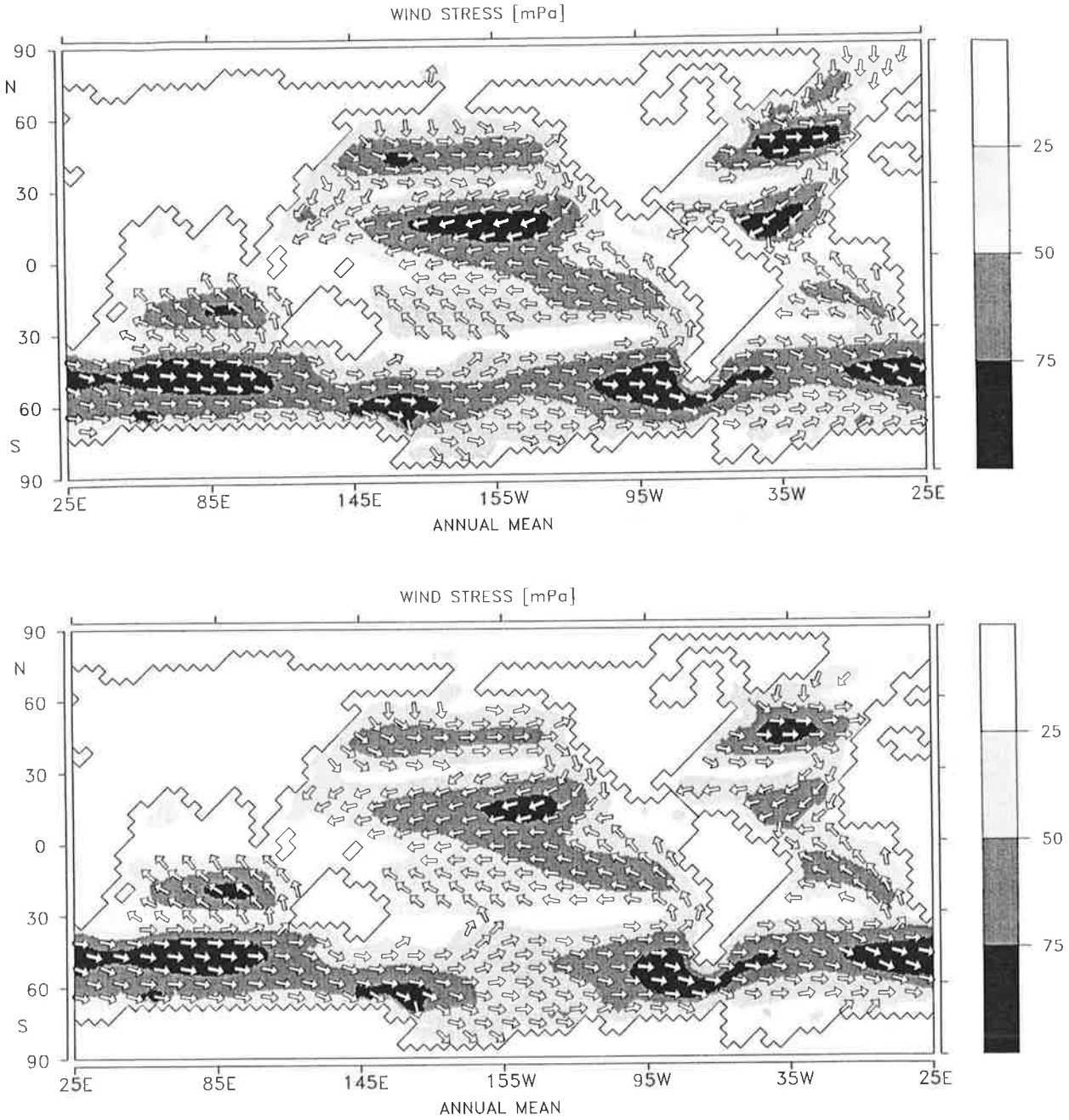

Figure 16: Annual mean wind stress field of experiments MINC (a) and CTRL (b). The magnitude of the wind stress vector is indicated by the shading, the direction by the arrows. Results are for the final decade (years 241-250) of experiments.

Greenland current is increased. This wind-driven feedback tends to compensate for the effect of the changed overturning circulation in case of suppressed NADW formation. It also tends to allow reinitiation of NADW formation, acting as a strong feedback mechanism stabilizing the conveyor belt mode of the thermohaline circulation. This was shown by Mikolajewicz (1996) in an OGCM coupled to a simple atmosphere model.

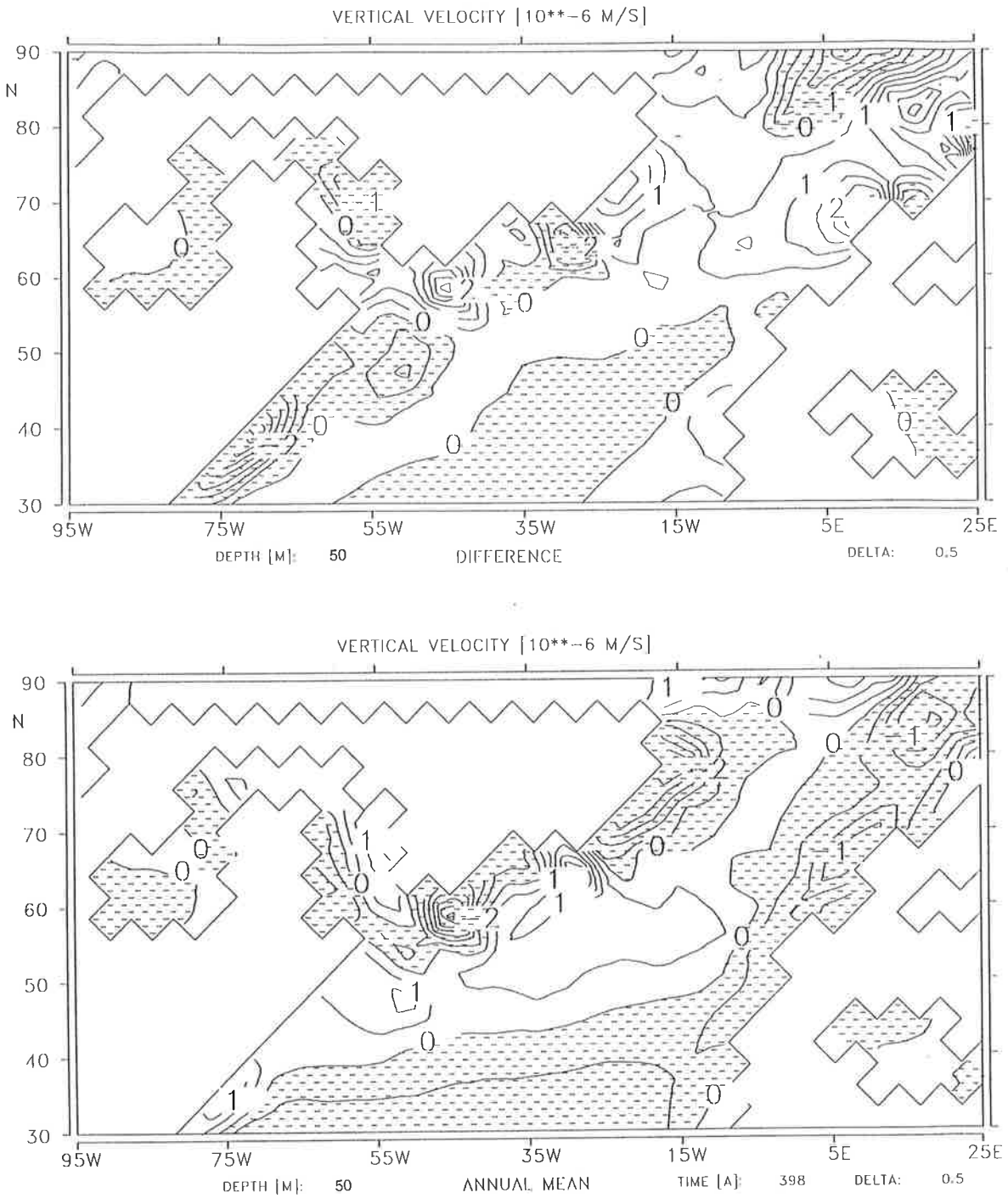

Figure 17: (a) Difference of vertical velocities between experiments MINC and CTRL; shading indicates negative values. C.I.: 5×10^{-7} m/s. (b) Annual mean vertical velocity between first and second layer of ocean model (z = 50 m) of control run CTRL. C.I.: 5×10^{-7} m/s.

3.1.4 Changes in freshwater fluxes

Due to the strong changes in the atmospheric circulation, the water budgets of experiments MINC and CTRL exhibit some remarkable differences. Figure 18a shows the difference in

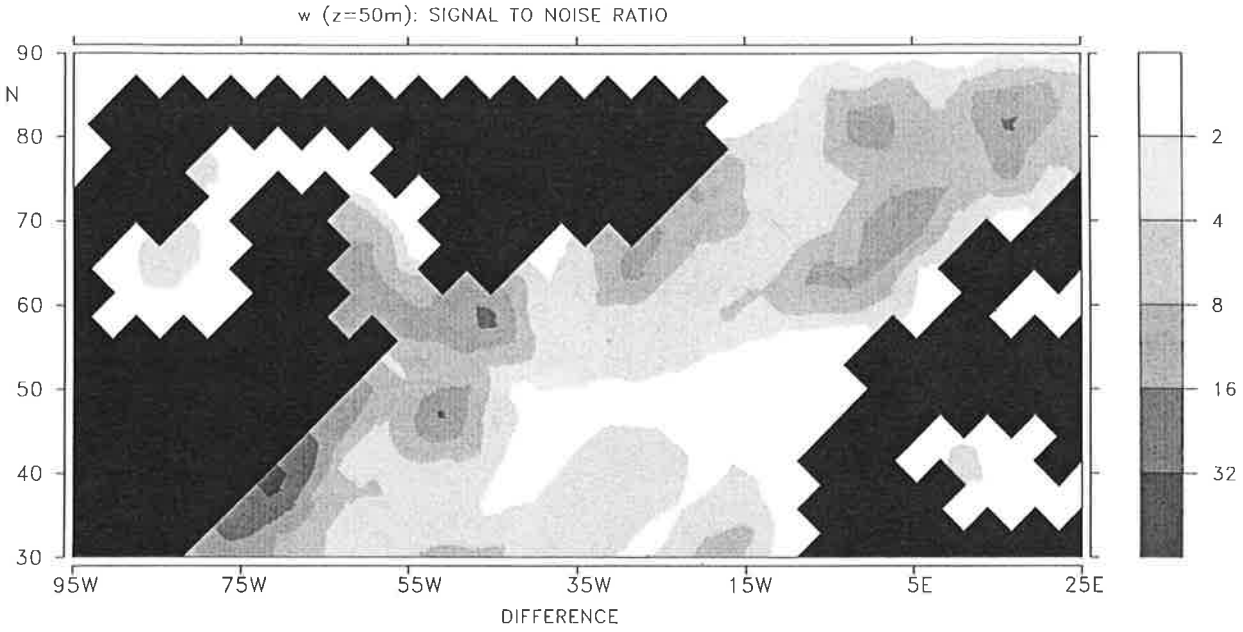

Figure 17: (c) Signal-to-noise ratio (absolute signal strength divided by standard deviation of decadal means from experiment CTRL) of the difference of the vertical velocities between experiments MINC and CTRL. Results are for the final decade (years 241-250) of experiments.

annual mean atmospheric net freshwater flux (precipitation minus evaporation) between the two experiments, Fig. 18b the corresponding difference in precipitation. Not surprisingly, given the changes in SST and near-surface air temperature, the strongest differences can be seen in the Atlantic. The strong dipole pattern in the equatorial Atlantic reflects the southeastward shift in the position of the Atlantic ITCZ and the precipitation maximum associated with it. This shift – a consequence of the oceanic heat transports being modified by a collapsed conveyor belt circulation – is in accordance with the changes in the positions of the Hadley cells.

Another striking feature is the large area of positive precipitation minus evaporation anomalies over the North Atlantic. This area has less evaporation in experiment MINC (up to 80 mm/month), caused by lower sea surface temperatures. The change in the precipitation rate in the North Atlantic north of 30°N is relative small. Except for the western part of the North Atlantic, precipitation is generally less (by typically 10 to 20 mm/month) in experiment MINC than in the control run, which partly cancels out the effect of the lower evaporation. The precipitation in West Africa south of the Sahara also tends to be lower. The reduction, especially in the Sahel zone, is small (about 10 mm/month), but in this dry area constitutes an important climate change. Another interesting feature of the hydrological cycle is the strong decrease in precipitation over Greenland during the meltwater experiment.

The overall effect of the changes in freshwater fluxes is a larger net gain of freshwater of the ocean in the case of a collapsed thermohaline circulation of 0.04 Sv in the North Atlantic (north of 30 °N). This enhanced northward transport of water vapour in the atmosphere is consistent with the increased cyclone activity and the larger meridional temperature gradient. The additional input of freshwater to the North Atlantic reduces the surface salinity there

even further and thus acts as a feedback process destabilizing the conveyor belt circulation and stabilizing circulation patterns without NADW. This effect was pointed out before by Nakamura et al. (1994).

3.1.5 Statistical significance

We tested the changes in the surface-forcing quantities of the ocean (wind-stress, net heat and freshwater flux, SST, and vertical velocity at 50 m as a proxy for wind-stress curl) for their statistical significance. As we are looking at a difference between ten-year means, we are comparing the differences between MINC and CTRL in the same decades with differences between different decades of CTRL. Assuming the decades to be independent, we have computed the standard deviation of differences between decadal means of the control run CTRL. The potentially largest errors in the estimate of the "noise" are probably the relatively small number of independent realizations in the control run or a hidden autocorrelation between adjacent decades. We are testing the hypothesis that our signal (differences between MINC and CTRL) could be explained by decadal variability in the CTRL experiment. If the signal to noise ratio is large, this hypothesis has to be rejected and the signal must be caused by the meltwater input. The data from the control run were detrended before computing the decadal means to avoid the effect of model drift.

As a typical example we show the results of the test of the vertical velocities below the first level at 50 m depth, which is essentially determined by the curl of the applied wind-stress-forcing field divided by the Coriolis parameter. Figure 17c depicts the signal-to-noise ratio of the vertical velocity signal shown in Fig. 17a in the northern North Atlantic. Almost the whole GIN-Sea shows a signal-to-noise ratio larger than two, with extreme values exceeding 16 standard deviations. Thus the signals in the shaded areas are with a probability of at least 95%, due to the meltwater input and not the result of internal variability of the coupled model. The results for the other tested quantities look qualitatively similar and all the features discussed in the text were significant at least on the 95% values, and in most cases were considerably higher.

3.2 Continued experiments with reduced meltwater input

As mentioned before, the ocean thermohaline circulation is – due to the prescribed meltwater input and the long time scales involved – certainly not in an equilibrium. From the previous experiment we identified four important feedback mechanisms influencing the stability of the achieved pattern of thermohaline overturning: the advection feedback and the increased atmospheric freshwater transport to the North Atlantic tend to keep the system in a circulation pattern similar to the one achieved at the end of MINC, whereas the effect of the surface cooling on the density and the increased upwelling of deep salty water in the Norwegian Sea, combined with the increased export of fresh surface waters through the East Greenland current into the North Atlantic, tend to drive the system back into a conveyor belt overturning pattern. To investigate whether the sum of these compensating feedbacks allows a stable second steady state mode of the thermohaline circulation without NADW to exist, we performed two additional experiments as indicated in Fig. 6a. Both experiments were started from the final state of experiment MINC.

In the first experiment MCON (Meltwater experiment CONtinued) the additional meltwater input was reduced instantanously to zero and kept at this value. This experiment was integrated for 200 years. In the second experiment MDEC (Meltwater input DECreasing) the

meltwater input was reduced linearly through time. After it had reached zero in year 500, the integration was continued without meltwater input for another 150 years. Time series of a

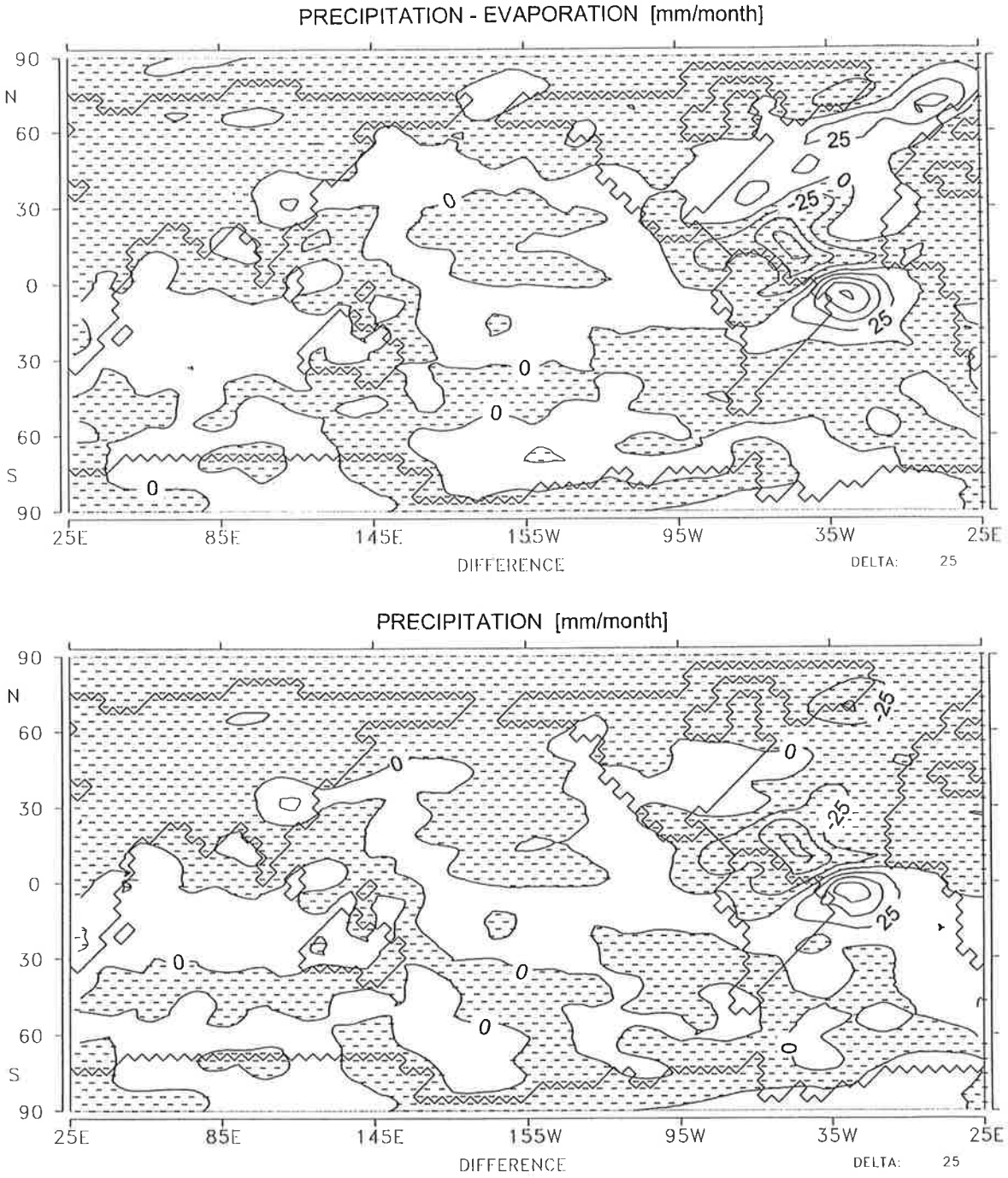

Figure 18: (a) Atmospheric freshwater flux (precipitation minus evaporation), difference between experiments MINC and CTRL. (b) Difference in precipitation between experiments MINC and CTRL. Shading denotes negative values, contour interval is 25 mm/month. Results are for the final decade (years 241-250) of both experiments.

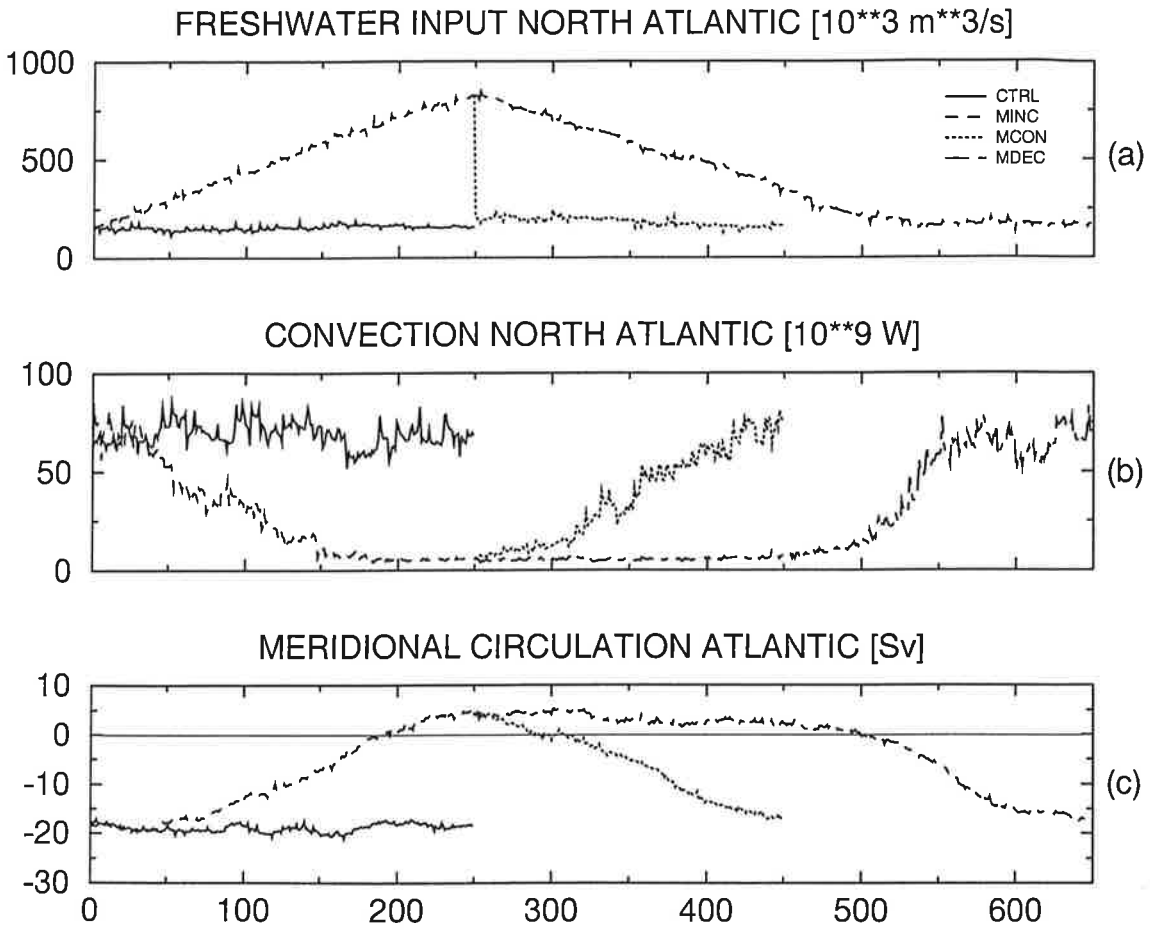

Figure 19: Time series (in years) of (a) prescribed meltwater plus freshwater input into the North Atlantic north of 30°N , (b) potential energy release through convection in the North Atlantic, (c) Meridional circulation ("overturning") at 60°S in Atlantic. Notation of experiments is given in upper right corner of (a). All data are annual means without further filtering.

few characteristic parameters from these experiments are shown in Figure 19. The difference in the net freshwater flux into the North Atlantic between the first years of MCON and the last years of CTRL is due to the differences in atmospheric water vapour transport discussed in the previous section.

After the meltwater input was switched off, the convection in the North Atlantic immediately started to recover in experiment MCON. It took about 120 years to reach a value almost as high as in the control run. The overturning at 1500 m depth at 30°S (an indicator of the outflow of NADW to the Southern Ocean) showed a matching, but somewhat delayed, response. At the end of the experiment, the NADW outflow was still weaker than the control run. In this experiment the NADW formation and the NADW outflow have both been suppressed for about 100 years. In experiment MDEC, the NADW formation was suppressed for a significantly longer period. It started to recover in year 460. Thus the formation of NADW has been suppressed for almost 300 years. Whereas one could argue that the deep thermo-

haline circulation of the Atlantic in MCON had not sufficient time to rearrange, this is rather unlikely to be the case in MDEC. As in the previous experiment, it took about 100 years for the convection to reach the strength of the control climate after the onset. Again, the outflow of NADW at 30°S showed a similar, but delayed, behaviour. At the end of MDEC, the rate of change of the outflow was significantly reduced, but it was still not in a steady state. Other integral parameters behaved roughly the same way. The overall circulation at the end of both experiments was clearly of the conveyor belt type and both experiments were approaching the climate of the control run. Convection, sea-surface temperature, surface velocities and sea-ice cover (none shown) reacted very much like the ones presented in section 2 for the control run. In neither experiment, the model could reach a stable climate that showed a thermohaline circulation pattern significantly different from the one maintained in the control run. Due to the enormous requirements in computer time, we could not run the experiments until a real steady state was achieved, this would have required several thousand years of additional integration time.

A number of other attempts to reach a stable mode without NADW by adding of instantaneous salinity anomalies had similar results to experiment MCON. For example, in one experiment salinity anomalies sufficient to reverse the meridional density gradient in all levels were added to the Atlantic. In another, the salinity of the top 112.5 m in the North Atlantic was halved; it took about 200 years for the NADW formation to resume.

3.3 Sensitivity to flux correction

We have discussed the effect of realistic feedbacks (advection and freshwater destabilizing, cooling and Ekman suction stabilizing) on the stability of the conveyor belt circulation. The coupled model might of course also have artificial feedbacks. The prime suspect is the flux correction, an artificial adjustment for all relevant variables at the ocean-atmosphere interface. This adjustment was necessary to suppress substantial climatic drifts caused by inconsistencies in the ocean and atmosphere subsystems (see section 2). The applied flux corrections vary geographically and through the seasonal cycle, but do not have interannual variations and are independent of the temporal variations of the model's climate. The flux correction of the heat flux, especially, extracted large amounts of heat from the surface of the ocean (up to annual mean 75 W/m^2) in the NADW formation regions of the control run. We wanted to test whether the heatflux correction affected our experiments on the stability of the thermohaline circulation.

It turned out that, without any heat flux correction, the model drifted very fast into a rather unrealistic state. However, the drift was comparatively small in the North Atlantic, so, in the next experiment we switched off the heat flux correction in the North Atlantic north of 45°N and increased it to its original values linearly between 45°N and 30°N. The annual mean heat flux correction in the North Atlantic is characterized by a large band of oceanic heat gain that covers the whole North Atlantic up to 60°N. The areas of deep-water formation (GIN-Sea, Labrador-Sea) release heat from the ocean, especially in winter. Amplitudes rarely exceed ± 200 W/m^2, respectively (not shown). However, the overall change implied in the oceanic heat transport due to the change in flux correction was small, corresponding to a net heat loss in the North Atlantic of 0.1 PW.

Starting from the initial state of the control run, we performed a spinup of 100 years to allow the system to adapt to the changes in forcing. We found both the residual drift of the model and its climate to be tolerable, so repeated some of the meltwater experiments with

this model without any heat flux correction in the North Atlantic. A schematic diagram of the experiments is shown in Fig. 6b. The names of the experiments are the same as the original model, with an N at the end to denote the modified model. At the end of a 250-year-long control run, the conveyor belt circulation had slightly weakened with an outflow of 16 Sv of NADW to the Southern Ocean (18 Sv in the original model). The overall oceanic heat transport of the Atlantic did not change significantly.

The impact of a smaller heat flux correction on the climate of the model is demonstrated in Figure 20. The zonally averaged near-surface air temperature differences between the control runs of the two model versions CTRLN and CTRL are presented for seasonal means of DJF and JJA. The lower heat gain of the ocean in the midlatitudes of the experiments without North Atlantic heat flux adjustment induces lower SSTs and thus lower near-surface air temperatures in the northern hemisphere. The largest differences of the zonal mean temperatures occur in winter above the sea (less than -4°C). The effect in summer is much weaker. Above the land areas of the middle and higher northern latitudes the decrease in near-surface air temperature is about 1°C. The comparably small regions of the former additional heat release of the ocean through corrected fluxes (GIN-Sea, Labrador Sea) appeared not to have a heating effect on the SST and near-surface air temperature, probably because these areas were strongly affected by sea-ice production. Note that the southern hemisphere south of 30°S during both seasons is slightly warmer for the experiment without North Atlantic heat flux adjustment than for the experiment with.

In the meltwater experiments we again increased the meltwater input linearly over 250 years up to 0.625 Sv (MINCN) and switched off the meltwater input instanteously thereafter (MCONN). The sequence of these experiments is shown in Fig. 6b. Figures 21a,b illustrate the time series of the strength of convection in the North Atlantic and the meridional circulation in the South Atlantic. Experiments CTRL and MINC/MCON have been explored in detail in the preceding sections. The two meltwater release experiments MINC and MINCN, as well as the subsequent instantaneous meltwater switch-off experiments MCON and MCONN, are quite similar in their overall physical behaviour. Nevertheless, a few notable differences became evident in the heat release of the North Atlantic to the atmosphere. In experiment MINCN the heat release in subpolar regions was lower due to the missing heat loss as prescribed by the flux correction. As a consequence, the reduced heat loss did not let the sea-ice thickness grow as much as in experiment MINC. This had no further consequences on the global circulation, however. The pattern of change in SST at the end of experiments MINCN and CTRLN was very similar to the respective pattern of the original model, but with slightly weaker amplitude. The maximum change was reduced slightly to 8°C (8.5°C in the original experiment). This is consistent with the slightly colder SSTs in the North Atlantic due to the missing of the heat flux correction. Thus the potential for cooling is smaller, as the freezing point sets a lower bound for the achievable negative SST anomalies. When the meltwater discharge was switched off (Exp. MCON and MCONN), both ocean circulations returned to their control state within roughly 200 years.

The experiments revealed only weak sensitivities of the global climate system and, moreover, of the stability of the thermohaline ocean circulation on modifications of the northern North Atlantic heat flux correction. Neither the current climate states nor the unstable modes of circulation showed any fundamental differences in the experiments with and without North Atlantic heat flux adjustment. Thus we consider it to be extremely unlikely that the convection in the North Atlantic resumed in our meltwater experiment because of the artificial effect of the heat flux correction.

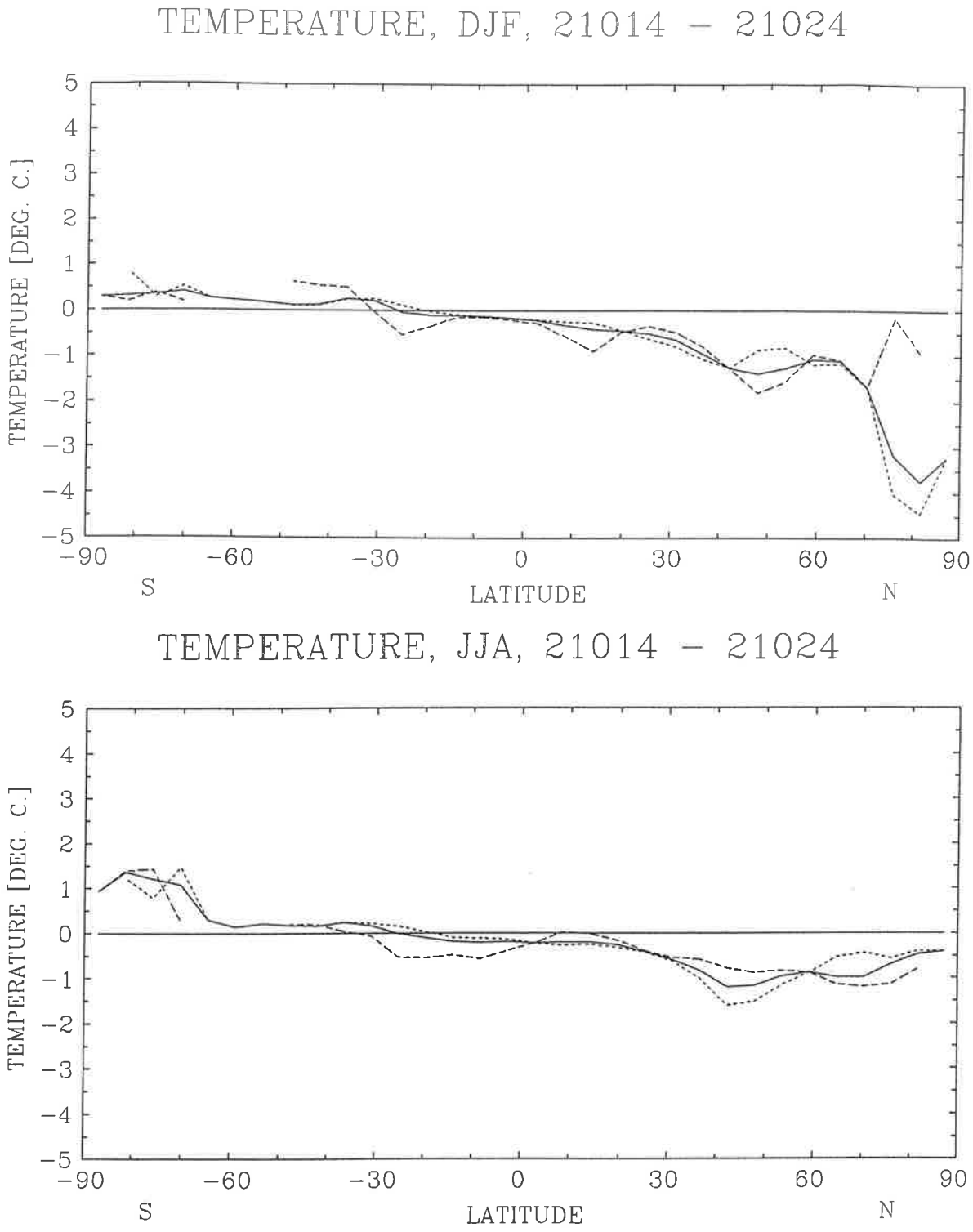

Figure 20: Differences of zonal mean near-surface air temperature for DJF (a) and JJA (b) between experiments CTRLN and CTRL. Results are for the final decade (years 241-250) of experiments. Solid line: total, dashed line: land, dotted line: ocean.

4 Discussion

The atmospheric response of our coupled model to an ocean circulation with suppressed NADW formation is in many aspects rather similar to the second steady state in the MS88

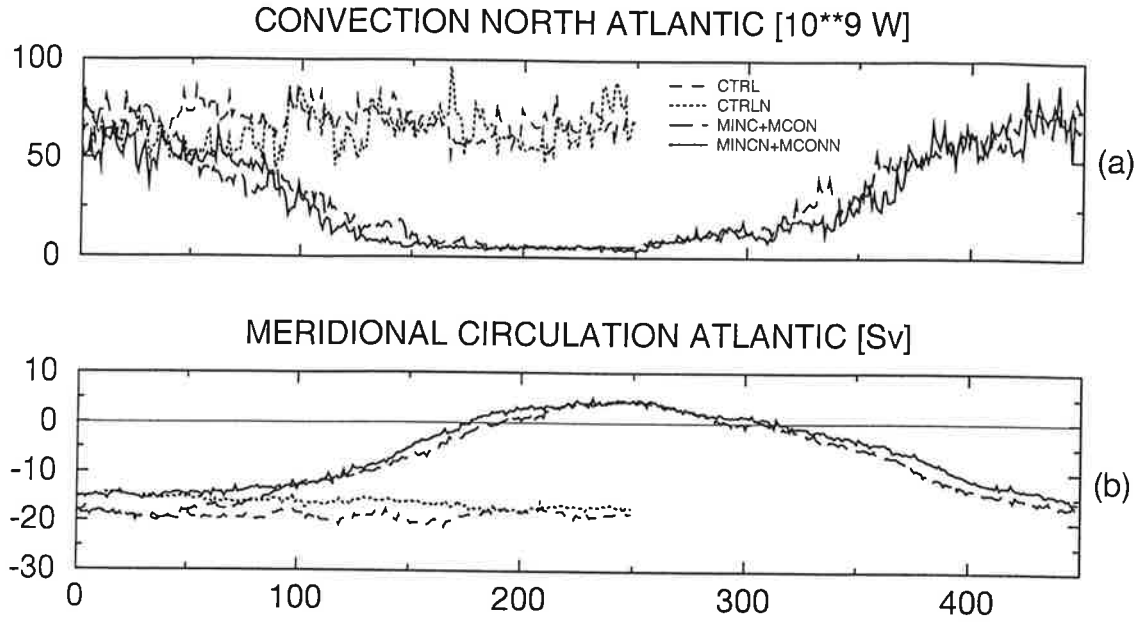

Figure 21: Time series (in years) of experiments with and without North Atlantic heatflux correction. (a) Potential energy release through convection in the North Atlantic, (b) Northward transport at 30°S in the Atlantic below 1500 m. Notation of experiments is given in (a). All data are annual means without further filtering.

model with annual mean insolation, characterised by missing NADW formation. The patterns of the annual mean response in SST are very similar. The maximum in the SST response in MS88 is 7°C; in our model 8.5°C. The maximum in MS88 is a band reaching from the Irminger Sea to the Scandinavian coast, whereas in our case it is shifted towards the European coast. The two models show a similar cooling in the North Pacific, though somewhat stronger in our model. The difference pattern in the near-surface air temperature is similar, with the maximum anomaly shifted further north than the maximum of the SST anomaly. Here the difference in the amplitude is much more pronounced. Whereas the maximum anomaly in the MS88 paper is below 10°C, our model has a maximum of 22°C, with significant higher values in northern hemisphere winter. This is consistent with the difference in northward oceanic heat transport in the Atlantic. Both models seem to underestimate this quantity considerably. Whereas our model has an Atlantic heat transport in the control run at 30°N of 0.7 PW, the MS88 model has a heat transport below 0.45 PW (estimated from their Fig. 19). Hall and Bryden's (1982) estimate at 25°N is 1.2 PW, Roemmich's (1980) at 36°N is 0.8 PW. In the case of a collapsed conveyor belt circulation both models have an Atlantic heat transport at 30°N of roughly 0.1 PW. Thus the change in heat release to the atmosphere is almost twice as strong in our model than in the MS88 model, so it is not surprising to see larger anomalies in the atmospheric response in our model. The difference in the oceanic heat transport can at least partly be attributed to the thermohaline overturning being about twice as strong in our model than in the MS88 model. The use of annual mean insolation in the MS88 simulation might also contribute to a weaker response, as this might lead to a significant underestimation of the ice albedo effect. The prescription of fixed cloud cover

should reduce the temperature response in the MS88 model, as our model shows a noticeable reduction in winter-time cloud cover over the Arctic, which amplifies the wintertime cooling.

The patterns of response of the atmospheric circulation to changes in the two models surface temperature agree surprisingly well, but the amplitude is considerably stronger in our model. The MS88 model shows the same shift in the position of the Hadley cells towards a symmetric (with respect to the equator) circulation in the case of a collapsed conveyor belt circulation. The structure of the response patterns in the 500 hPa geopotential height field is rather similar. Both models predict a deepening of the Icelandic and Aleutian lows, but MS88 get only 40% of our response.

The pattern of the response in precipitation is also similar in the two models. Both models show the southward shift of the equatorial rainbelt in the Atlantic, and reduced precipitation over most of the Atlantic and east Greenland. In contrast to many other quantities, the changes in precipitation seem to be considerably larger in the MS88 model – often by a factor between 1.5 and 2 – than in our model. Some of the precipitation changes in both models coincide reasonable well with geological and glaciological evidence. Alley et al. (1993) report an abrupt increase in Greenland snow accumulation rate in the GISP2 ice core at the end of the Younger Dryas cold episode. Street-Perrot and Perrot (1990) report on the climate in North Africa being dryer than today during the Younger Dryas. This fits with the reduced precipitation in both models in this area.

The cooling in former deepwater convection areas with the input of meltwater counteracts the effect of the reduced salinities in the density structure. This has been pointed out in a couple of recent OGCM-only experiments. The restoring boundary condition for temperature used in most experiments on the role of ocean in climate (e.g. Bryan, 1986, MM89, Marotzke and Willebrand, 1991, Weaver and Hughes, 1992) gives unrealistic high sensitivities for the response of the thermohaline circulation against perturbations (e.g. Zhang et al., 1994, MM94, Rahmstorf and Willebrand, 1995). The modifications in the upper boundary conditions changed the amplitude of the SST response moderately, but had strong effects on the stability of the thermohaline circulation. This temperature/heat flux feedback is a strong stabilizer for the conveyor belt thermohaline circulation, largely compensating for the destabilizing advective feedback on the salinity fields.

The destabilizing effect of changes in atmospheric moisture transport has been discussed by Nakamura et al. (1994) in a simple one-hemisphere coupled atmosphere-ocean boxmodel. The enhanced meridional temperature gradients in the case of small oceanic poleward heat transport induce an intensification of the cyclonic activity (see Fig. A13). Together with the increased temperature gradients in the atmosphere this leads to an amplification of the atmospheric poleward moisture transport, resulting in stronger net precipitation (both evaporation and precipitation are actually reduced due to the colder SSTs) in the North Atlantic and Arctic oceans and a further dilution of the sea-surface salinity in these areas. The overall change in water vapour transport over the Atlantic and its drainage areas in our model was 0.04 Sv at 30°N; the net freshwater input into the Atlantic and Arctic north of this latitude was 0.16 Sv in the control run. Nakamura et al. (1994) estimated this effect to be between 0.035 and 0.045 Sv.

The stronger upwelling due to the strong cyclonic circulation in the GIN-Sea in the case of suppressed NADW-formation tends to bring warmer and saltier water (compared with surface water diluted by meltwater at the freezing point) to the surface. Given a change in the upwelling rate of 0.5×10^{-6} m/s, this corresponds to a net evaporation of almost 40 mm/month at the surface for every psu salinity difference between the first and the second

layer. Examples of stable modes of the thermohaline circulation without NADW formation typically show a rather high vertical gradient in salinity in the northern North Atlantic (e.g. Bryan 1986, MS88), with a difference of several psu between surface and intermediate waters. The additional heat brought to the surface by the upwelling, together with the atmospheric circulation pushing the ice away from the center of the cyclonic circulation, tends to create an ice-free area in the Norwegian Sea. Once this ice-free area exists, local evaporation will increase significantly and further amplify the effect of the upwelling. The enhanced East Greenland Current exports relatively fresh surface waters into the North Atlantic. The wind-driven changes in circulation represent a strong feedback stabilizing the present mode of ocean circulation. This effect is not discussed in the MS88 paper, but given the similarity in the response in sea level pressure and geopotential height in the two models, it should exist in their model as well, but with significantly smaller amplitude because its atmospheric response is significantly weaker. Mikolajewicz (1996) showed in experiments with on OGCM coupled to a nonlinear energy balance model that the mode without NADW became weakly unstable, when the wind-stress feedback was included.

We identified four feedbacks affecting the stability of the present mode of thermohaline circulation: two (the advection and the water-vapour transport feedback) are destabilizing; the other two (the cooling and the upwelling) are stabilizing. They largely compensate each other. From the experiments with decreasing, and finally vanishing, meltwater input we can see that the thermohaline circulation does not settle in a stable mode without NADW formation, even if the formation of NADW has been suppressed for several hundred years. In all our experiments (including those with added instantaneous negative salinity anomalies as strong as reducing the surface salinity of the top two levels in the North Atlantic to 50% of the value of the control run) the thermohaline circulation returned to a conveyor belt type. Although all experiments are much too short to really achieve a steady state, we expect that the overturning pattern in the Atlantic would finally settle in a state similar to the control run.

On the basis of our experiments we cannot exclude the existence of a stable mode without NADW formation in our model (the exact proof is practically impossible in GCMs), but we think we can exclude the possibility that this mode is the preferred mode of the system, unlike the behaviour of most OGCMs under traditional "mixed boundary conditions". Our results strongly indicate that the conveyor belt type of overturning is the preferred mode of the thermohaline circulation of our model, as the sum of the stabilizing feedbacks for this type is larger than the sum of the destabilizing feedbacks. It turned out that especially the upwelling feedback, which has been neglected in most previous studies, is very important in reestablishing the conveyor belt circulation.

The results of the experiments without heat flux correction in the North Atlantic make it extremely unlikely that the strong stability of the conveyor belt circulation in our model is an artefact of the heat flux correction. The correction for the freshwater flux adds freshwater to the northern North Atlantic and the GIN-Sea, so, if it has an effect on our results, it would be expected to destabilize, rather than stabilize the conveyor belt type of overturning. However, we cannot exclude the possibility that our results are affected by other components of the flux correction. In future models we expect the uncertainties associated with the flux correction to become significantly smaller as the models improve.

The periodically synchronous coupling was tested by Voss et al. (1996) and Voss and Sausen (1996). It gave satisfactory results for climate changes on time scales of decades. For shorter time scales the temporal evolution of the response is distorted significantly, with a

strong damping of processes with periods below 4 to 5 years and an amplification of periods around 10 to 20 years. We reran shorter periods of the scenarios without this acceleration technique but did not find significant differences. As the dominant time scale of the response in our model was of several decades, we do not expect the periodically synchronous coupling technique to be a major source of error in the experiments presented here. We cannot, however, exclude the possibility that, without this acceleration technique, the transitions between circulation patterns with and without NADW might have been more abrupt.

Due to the coarse resolution of the models, many processes had to be parameterized in the two subcomponents of the model, some of them in a rather crude way. In the ocean the most important processes of that kind include eddies, convection and sea-ice; in the atmosphere the cloud parameterizations are a likely source of uncertainty. Whereas the parameterizations give a reasonably realistic climate, they might be inadequate for climate change.

Another potential source of error is the coding, but this is almost unavoidable in codes of this complexity, and we did our best to test the model.

It must be stressed once more that our simulations are too short for the coupled system to reach real steady states. Whereas some of the integrations were long enough for the variations in the surface properties of the ocean – and thus the atmosphere – to reach a quasi-steady state (meaning that both the climatology and the variability are in a statistical steady state), the deep ocean properties were still far away from being in equilibrium.

Our ECHAM3/LSG model shows a higher stability of the conveyor belt mode of the thermohaline circulation than the annual mean model of MS88 and most ocean-only models. We think the difference in the behaviour can be explained by the weakness of stabilizing atmospheric feedbacks in the MS88 model or their total neglect in ocean-only models. The atmospheric response in the MS88 model is typically only one half of the response in our model. As the atmospheric feedbacks had a tendency to stabilize the conveyor belt circulation, this weaker atmospheric response could be responsible for the differences in stability. Besides that, the conveyor belt circulation in our model is about twice as strong as in the MS88 model. This, too, should definitely have a significant effect on its stability. Recently, Manabe and Stouffer (1995), with a newer version of their coupled OAGCM, investigated the effect of meltwater input into the North Atlantic as well. They prescribed an input of 1 Sv over 10 years and continued the experiment. As a result they got a temporal strong reduction of NADW-formation, but afterwards the conveyor belt circulation recovered.

From investigations with simpler models we know that many parameters determine whether multiple steady states of the thermohaline circulation exist, and if so, how stable they are. In simple Stommel-type box models (Stommel, 1961) it is straightforward to compute necessary conditions for the existence of multiple steady states. Stocker and Wright (1991) in a zonally averaged 2.5D model and MM94 in an OGCM have shown hysteresis curves of the thermohaline circulation depending on freshwater fluxes and how the surface heat flux boundary condition is formulated. The possibility of a second (or even third) steady state of the thermohaline circulation depends in a rather nonlinear way on these parameters. Parameters that must be expected to be of importance are, for example, the freshwater transport of the model and the one implied by the flux correction, the strength of the meridional overturning in the model, details of parameterizations at the atmosphere-ocean boundary (including the sea-ice model and the coupling technique, especially the flux correction problem).

The potentially nonlinear dependence of the results on the values of the single parameters raises the question of whether our model is at the correct point in parameter space. Due to the complexity of the model, the only way to obtain reliable information would be to make an

extensive set of experiments with different parameters to find out whether the model is close to a bifurcation point. This approach is prohibitively expensive. A way to get at least some information about the behaviour of the model is to fit a simple atmosphere model coupled to an OGCM to the OAGCM and explore the potential stability behaviour with extensive experiments in this model, together with a few selected experiments utilizing the fully coupled OAGCM. The first steps taking this approach have already been made (Mikolajewicz, 1996).

5 Summary and conclusion

A fully coupled OAGCM with seasonal cycle has been used to investigate the response of the climate system to a prescribed meltwater release into the Labrador Sea. An input of 0.38 Sv was sufficient to suppress the formation of NADW and finally reverse the thermohaline circulation of the Atlantic, leaving AABW the only water mass to fill the deep Atlantic. The overturning pattern without NADW did not appear to be a stable mode of this model and the conveyor belt circulation recovered about 150 years after the addition of meltwater ended.

The surface response to the meltwater release is – as expected – strongest in the North Atlantic, leading to a strong reduction in both SST and air temperatures. The cooling extends over Eurasia into the North Pacific. A southward shift of the Atlantic ITCZ is connected with a Hadley circulation almost symmetric around the equator. The atmospheric response is typically much stronger in the northern hemisphere winter than in summer.

During the meltwater experiments we could identify four major feedbacks that influence NADW formation, but act in opposite directions, and thus partly cancel each other out:

1. The changes in the overturning leading to reduced advection of saline, low-latitude surface water and significantly longer residence times of the surface waters in the high-latitude areas of the North Atlantic and Arctic, with net precipitation lead to a further reduction of the surface salinity in the northern North Atlantic and thus increase the vertical stability of the water column.

2. The reversed thermohaline circulation reduces the northward heat transport of the Atlantic from 0.7 to 0.1 PW. As a consequence, the SST shows a marked cooling in the whole North Atlantic, with up to 8.5°C (annual mean) close to the European coast. The changes in annual mean near-surface air temperature are even larger, with up to 22°C over regions now covered by sea-ice. The changes are larger in winter than in summer. The cooling of the sea surface increases the surface density, counteracting the effect of the freshening. The reduced stability of the water column allows enhanced mixing with the underlying, more salty, water masses.

3. The increased meridional temperature gradient over the Atlantic leads to increased cyclonic activity over the North Atlantic and increased northward atmospheric water vapour transport. This additional freshwater input to the North Atlantic dilutes the surface salinity and increases the stability of the water column.

4. In the atmosphere the deepening of the trough over the northern North Atlantic leads to an intensification of the cyclonic circulation in the subpolar gyre and intensified upwelling through Ekman-suction. The intensified East Greenland Current exports fresh surface waters to the North Atlantic. This wind-driven feedback turned out to be rather strong and its inclusion to be important for the breakdown of the stable stratification in the Norwegian Sea and the onset of NADW formation.

Whereas the patterns of the atmospheric response of our experiments with the ECHAM3/ LSG OAGCM are very similar to the response in the MS88 coupled OAGCM with annual mean insolation, the amplitudes of the stabilizing feedbacks are considerably stronger in our model. Due to the nonlinearity of the problem, this quantitative difference in the strength of single feedbacks (typically by a factor of two) leads to a qualitative difference in the response of the coupled system. Thus the conveyor belt circulation is definitely the preferred, and probably also the only, mode of thermohaline circulation in our OAGCM, in contrast to the results of MS88 and most ocean-only models.

The results of our experiments have important implications for the understanding of climate history since the last glacial maximum. The formation rate of NADW seems to have been substantially weaker during the last glacial maximum than today, as can be inferred from the distribution of δ13C in the Atlantic presented by Duplessy (1981).

During the process of deglaciation, there are indications that the formation rate of NADW underwent strong changes. A warm period with a peak in meltwater discharge (Fairbanks, 1989) was followed by the Younger Dryas cold spell. There are some indications that NADW formation was totally suppressed, or at least was much weaker, than at present (e.g. Boyle and Keigwin, 1987). The end of the Younger Dryas cold spell was rather abrupt, as can be inferred from ice core data (Dansgaard et al., 1989). Deepwater formation recovered and was not significantly affected by another meltwater peak. Assuming that the thermohaline circulation of the ocean has multiple steady states leads to the question of why the climate system since the last glacial maximum was most of the time in the mode with NADW. The meltwater spikes should have been sufficient to bring the system into the mode without NADW formation and one would need a strong perturbation to bring the system again into the present mode of overturning. One explanation could be that the second meltwater peak came mostly from Antarctica, and thus reduced AABW formation. This finally could lead to the onset of NADW formation, as in a steady state the formation rate of these water masses seems to be inversely correlated (cf. model results from Maier-Reimer et al., 1993). The explanation becomes much easier if the system is in a parameter regime where only one steady state is stable and where the mode without NADW is weakly unstable, as demonstrated by Wright and Stocker (1993) with their 2.5-dimensional ocean model coupled to an EBM. In this case the explanation as to why the climate system has been most of the time in a conveyor belt type ocean circulation mode becomes straightforward: the system has only one stable mode and returns to it (with some delay) when the perturbations are not (or no longer) strong enough to destroy this circulation pattern. Lehman et al. (1993) have shown that such a scenario is consistent with the history of the δ18O changes discernible in marine sediment cores.

Acknowledgements: We appreciated the comments of Ulli Cubasch, Mojib Latif and Ernst Maier-Reimer on this manuscript. Marion Grunert and Stephan-S. Schultz helped with the plots. We thank Vivienne Mawson for improving the clarity of the language. This work was funded by the Deutsche Forschungsgemeinschaft (through the Sonderforschungsbereich 318) and by the German WOCE program of the BMFT. The proofreading of the manuscript was funded by CSIRO.

References

Alley, R.B., D.A. Meese, C.A. Shuman, A.J. Gow, K.C. Taylor, P.M. Grootes, J.W.C. White, M. Ram, E.D. Waddington, P.A. Mayewski and G.A. Zielinski, 1993, Abrupt increase in Greenland snow accumulation at the end of the Younger Dryas event, Nature, 362, 527 - 529.

Arakawa, A. and V.R. Lamb, 1977, Computational design of the basic processes of the UCLA General Circulation Model, Methods Comput. Phys., 17, 173 - 265.

Baumgartner, A. and E. Reichel, 1975, Die Weltwasserbilanz/The world water balance (bilingual), Oldenbourg, 179 pp.

Blackmon, M.L., 1976, A climatological spectral study of the 500 mb geopotential height of the northern hemisphere. J. Atm. Sci., 33, 1607-1623.

Bond, G.W., W. Broecker, S. Johnsen, J. McManus, L. Labeyrie, J. Jouzel and G. Bonani, 1993, Correlations between climate records for North Atlantic sediments and Greenland ice core, Nature, 365, 143-147.

Boyle, E.A. and L.D. Keigwin, 1987, North Atlantic circulation during the last 20,000 years linked to high latitude surface temperature, Nature, 300, 35-40.

Broecker, W.S. 1991, The great ocean conveyor, Oceanography, 4, 79-89.

Broecker, W.S., D.M. Peteet and D. Rind, 1985, Does the ocean-atmosphere system have more than one stable mode of operation?, Nature, 315, 21-26.

Broecker, W., G. Bond, M. Klas, E. Clark and J. McManus, 1992, Origin of the North Atlantic's Heinrich events, Clim. Dyn. 6, 265-273.

Bryan, F., 1986, High latitude salinity effects and interhemispheric thermohaline circulations, Nature, 323, 301-304.

Cubasc, U., K. Hasselmann, H. Höck, E. Maier-Reimer, U. Mikolajewicz, B.D. Santer and R. Sausen, 1992, Time-dependent greenhouse warming computations with a coupled ocean-atmosphere model, Climate Dynamics, 8, 55-69.

Dansgaard, W., 1985, Greenland ice core records, Paleogeogr. Paleoclimatol. Paleoecol., 50, 185-187.

Dansgaard, W., J.W.C. White and S.J. Johnsen, 1989, The abrupt termination of the Younger Dryas climate event, Nature, 339, 532-534.

Dorman, C.E. and R.H. Bourke, 1981, Precipitation over the Atlantic Ocean, 30°S to 70°N, Monthly Weather Rev., 109, 554-563.

Duplessy, J.C., 1981, North Atlantic deep water circulation during the last climate cycle, Bulletin de l' Institut de Geologie du Bassin d 'Aquitaine, Talence, Environements sedimentaire de l'Atlantic Nord au Quaternaire, 31-32, 379-391.

Fairbanks, R.G., 1989, A 17,000-year glacio-eustatic sea level record: Influence of glacial melting rates on the Younger Dryas event and deep-ocean circulation, Nature, 342, 637-642.

Gates, W.L., J.F.B. Mitchell, G.J. Boer, U. Cubasch and V.P. Meleshko 1992, in J.T. Houghton, B.A. Callander and S.K. Varney (ed.), Climate Change 1992, Cambridge University Press, p. 95-134.

Gates, L., U. Cubasch, G.A. Meehl, J.F.B. Mitchell and R.J. Stouffer, 1993, An intercomparison of the control climates simulated by coupled atmosphereocean general circulation models, SGGCM, WCRP-92, WMO-TD No. 574.

Gordon, A., 1986, Interocean exchange of thermohaline water, J. Geophys. Res., 91, 5037-5046.

Hall, M.M. and H.L. Bryden, 1982, Direct estimates and mechanisms od ocean heat transport. Deep-Sea Research 29A, 339-359.
Heinrich, H. (1988), Origin and consequences of cyclic rafting in the northeast Atlantic Ocean during the past 130,000 years, Quat. Res., 29, 143-152.
Hughes, T.M.C. and A.J. Weaver, 1994, Multiple equilibria of an asymmetric two-basin model, J. Phys. Oceanogr., 24, 619-637.
Isemer, H.-J. and L.Hasse, 1987, The Bunker climate atlas of the North Atlantic Ocean, 2, Springer Verlag, 252 pp.
Killworth, P.D., 1983, Deep convection in the world ocean, Rev. Geophys. and Space Phys., 21, 1-26.
Legates, D.R. and C.J. Willmott, 1990, Mean seasonal and spatial variability in global surface air temperature. Theo. appl. Climatol., 41, 11-21.
Lehman, S.J., D.G. Wright and T.F. Stocker, 1993, Transport of freshwater into the deep ocean by the conveyor, in: Ice in the climate system, edited by W.R. Peltier, pp. 187-209, Springer-Verlag.
Lenderink, G. and R.J. Haarsma, 1994, Variability and multiple equilibria of the thermohaline circulation associated with deep-water formation, J. Phys. Oceanogr., 24, 1480-1493.
Maier-Reimer, E. and U. Mikolajewicz, 1989, Experiments with an OGCM on the cause of the Younger Dryas, Proc. JOA 1988, 87-99.
Maier-Reimer, E., U. Mikolajewicz and K. Hasselmann, 1993, Mean circulation of the LSG OGCM and its sensitivity to the thermohaline surface forcing, J. Phys. Oceanogr., 23, 731-757.
Manabe, S. and R.J. Stouffer, 1988, Two stable equilibria of a coupled ocean-atmosphere model, J. Clim., 1, 841-866.
Manabe, S., K. Bryan and M.J. Spelman, 1990, Transient response of a global ocean-atmosphere model to a doubling of atmospheric carbon dioxide, J. Phys. Oceanogr., 20, 722-749.
Manabe, S. and R.J. Stouffer, 1993, Century-scale effects of increased atmospheric CO2 on the ocean-atmosphere system, Nature 364, 215-218.
Manabe, S. and R.J. Stouffer, 1995, Simulation of abrupt climate change induced by freshwater input to the North Atlantic Ocean, Nature, 378, 165-167.
Marotzke, J. and J. Willebrand, 1991, Multiple equilibria of the global thermohaline circulation, J. Phys. Oceanogr., 21, 1372-1385.
Marotzke,J. and P.H. Stone, 1994, Atmospheric transports, the thermohaline circulation, and flux adjustments in a simple coupled model, J. Phys. Oceanogr., 25, 1350-1364.
Mayewski, P.A., L.D Meeker, S. Whitlow, M.S. Twickler, M.C. Morrison, R.B. Alley, P. Bloomfield and K. Taylor, 1993, The atmosphere during the Younger Dryas, Science, 261, 195-197.
Mikolajewicz, U. and E. Maier-Reimer, 1990, Internal secular variability in an ocean general circulation model, Climate Dynamics, 4, 145-156.
Mikolajewicz,U., E. Maier-Reimer, T.J. Crowley and K.-Y. Kim, 1993, Effect of Drake and Panamanian gateways on the circulation of an ocean model. Paleoceanography, 8, 409-426.
Mikolajewicz, U., 1996, A meltwater induced collapse of the thermohaline circulation and its influence on the oceanic distribution of d14C and d18O, in preparation.
Mikolajewicz, U. and E. Maier-Reimer, 1994, Mixed boundary conditions in ocean general circulation models and their influence on the stability of the model's conveyor-belt, J. Geophys. Res., 99, 22633-22644.

Milankowitsch, M., 1930, Mathematische Klimalehre und astronomische Theorie der Klimaschwankungen, in: W. Köppen und R. Geiger (Eds.) Gebrüder Borntraeger, Berlin.
Nakamura, M., P.H. Stone and J. Marotzke, 1994, Destabilization of the thermohaline circulation by atmospheric eddy transports, J. Clim., 7, 1870 - 1882.
Power, S.B., A.M. Moore, D.A. Post, N.R. Smith and R. Kleeman, 1994, Stability of North Atlantic deep water formation in a global general circulation model, J. Phys. Oceanogr., 24, 904-916.
Rahmstorf, S. and J. Willebrand, 1995, The role of temperature feedback in stabilising the thermohaline circulation, J. Phys Oceanogr., 25, 787-805.
Rahmstorf, S., 1995, Multiple convection patterns and the thermohaline flow in an idealised OGCM, J. Clim., in press.
Rahmstorf, S., J. Marotzke and J. Willebrand, 1995, Stability of the Thermohaline Circulation, to appear in: The warm water sphere of the North Atlantic Ocean, edited by W. Krauß, in prep.
Rintoul, S.R., 1991, South Atlantic interbasin exchange, J. Geophys. Res., 96, 2675-2692.
Roeckner, E., K. Arpe, L. Bengtsson, S. Brinkop, L. Dümenil, M. Esch, E. Kirk, F. Lunkeit, M. Ponater, B. Rockel, R. Sausen, U. Schlese, S. Schubert, M. Windelbrand, 1992, Simulation of the present-day climate with the ECHAM model: Impact of model physics and resolution, Max-Planck-Institut für Meteorologie, Report No. 93, Hamburg, 171 pp.
Roemmich, D., 1980, Estimation of meridional heat flux in the North Atlantic by inverse methods. J. Phys. Oceanogr. 10, 1972-1983.
Rooth, C., 1982, Hydrology and ocean circulation. Prog. Oceanogr., 11, 131-149.
Sausen, R., K. Barthel and K. Hasselmann, 1988, Coupled ocean-atmosphere models with flux correction, Climate Dynamics, 2, 145-163.
Schlesinger, M.E., 1979, Discussion of a global ocean-atmosphere model with seasonal variation for future studies of climate sensitivity'. Dyn. Atmos. Oceans, 3, 427-432.
Schmitz, W.J., 1995, On the interbasin-scale thermohaline circulation, Review of Geophysics, 33, 151-173.
Stocker, T.F. and D.G. Wright, 1991, Rapid transitions of the ocean's deep circulation induced by changes in the surface fluxes, Nature, 351, 729-732.
Stommel, H.H., 1961, Thermohaline convection with two stable regimes of flow, Tellus, XIII, 224-230.
Street-Perrot, F.A. and R.A. Perrot, 1990, Abrupt climatic fluctuations in the tropics - the influence of the Atlantic Ocean circulation, Nature, 343, 607-612.
Voss, R., R. Sausen and U. Cubasch, 1996, Periodically-synchronously coupled integrations with the atmosphere-ocean general circulation model ECHAM3/LSG, in preparation.
Weaver, A.J. and M.C. Hughes, 1992, Stability and variability of the thermohaline circulation and its links to climate, Trends in Phys. Oceanogr., 1, 15-70.
Weaver, A.J. and E.S. Sarachik, 1991, The role of mixed boundary conditions in numerical models of the ocean climate, J. Phys. Oceanogr., 21, 1470-1493.
Wright, D.G. and T.F. Stocker, 1993, Younger Dryas experiments, in: Ice in the climate system, edited by W.R. Peltier, pp. 395-416, Springer-Verlag.
Zhang, S., R.J. Greatbatch and C.A. Lin, 1993, A reexamination of the polar halocline catastrophe and implications for coupled ocean-atmosphere modelling. J. Phys. Oceanogr., 23, 287-299.